The Amsterdam-St. Paul Plateau: A complex hot spot/DUPAL-flavored MORB interaction

Myriam Janin, Christophe C Hémond, Marcia Maia, Philippe Nonnotte, Emmanuel Ponzevera, K.T.M. Johnson

Geochemistry Geophysics Geosystems G3

Article
Volume 13, Number 9
28 September 2012
Q09016, doi:10.1029/2012GC004165
ISSN: 1525-2027

Published by AGU and the Geochemical Society

The Amsterdam–St. Paul Plateau: A complex hot spot/DUPAL-flavored MORB interaction

M. Janin
Université Européenne de Bretagne, 6 avenue Le Gorgeu, FR-29200 Brest, France

Domaines Océaniques, Université de Brest, CNRS, Institut Universitaire Européen de la Mer, Place Copernic, FR-29280 Plouzané, France

Now at Laboratoire de Géochimie Isotopique Environnementale, Université de Nîmes, CEREGE, UMR6635, 150 rue Georges Besse, FR-30035 Nimes CEDEX 1, France (myriam.janin@unimes.fr)

C. Hémond, M. Maia, and P. Nonnotte
Université Européenne de Bretagne, 6 avenue Le Gorgeu, FR-29200 Brest, France

Domaines Océaniques, Université de Brest, CNRS, Institut Universitaire Européen de la Mer, Place Copernic, FR-29280 Plouzané, France

E. Ponzevera
Département Géosciences Marines, Ifremer, FR-29280 Plouzané, France

K. T. M. Johnson
School of Ocean and Earth Science and Technology, University of Hawai'i at Mānoa, Honolulu, Hawai'i 96822, USA

[1] The Amsterdam–St Paul (ASP) oceanic plateau results from the interaction between the ASP hot spot and the Southeast Indian ridge. A volcanic chain, named the Chain of the Dead Poets (CDP), lies to its northward tip and is related to the hot spot intraplate activity. The ASP plateau and CDP study reveals that ASP plume composition is inherited from oceanic crust and pelagic sediments recycled in the mantle through a 1.5 Ga subduction process. The ASP plateau lavas have a composition (major and trace elements and Sr-Nd-Pb-Hf isotopes) reflecting the interaction between ASP plume and the Indian MORB mantle, including some clear DUPAL input. The Indian upper mantle below ASP plateau is heterogeneous and made of a depleted mantle with lower continental crust (LCC) fragments probably delaminated during the Gondwana break-up. The lower continental crust is one of the possible reservoirs for the DUPAL anomaly origin that our data support. The range of magnitude of each end-member required in ASP plateau samples is (1) 45% to 75% of ASP plume and (2) 25% to 55% of Indian DM within 0% to a maximum of 6% of LCC layers included within. The three end-members involved (plume, upper mantle and lower continental crust) and their mixing in different proportions enhances the geochemical variability in the plateau lavas. Consequently, the apparent composition homogeneity of Amsterdam Island, an aerial summit of the plateau, may result from the presence of intermediate magmatic chambers into the plateau structure.

Components: 16,800 words, 8 figures, 2 tables.

Keywords: DUPAL anomaly; Indian Ocean; Sr-Nd-Pb-Hf isotopes; ridge–hot spot interaction.

Index Terms: 3038 Marine Geology and Geophysics: Oceanic plateaus and microcontinents; 3621 Mineralogy and Petrology: Mantle processes (1038); 9340 Geographic Location: Indian Ocean.

Received 26 March 2012; **Revised** 22 August 2012; **Accepted** 23 August 2012; **Published** 28 September 2012.

Janin, M., C. Hémond, M. Maia, P. Nonnotte, E. Ponzevera, and K. T. M. Johnson (2012), The Amsterdam–St. Paul Plateau: A complex hot spot/DUPAL-flavored MORB interaction, *Geochem. Geophys. Geosyst.*, *13*, Q09016, doi:10.1029/2012GC004165.

1. Introduction

[2] The isotopic ratios of Sr, Nd, Pb and Hf of volcanic rocks in the oceans shed light on the source of the magmatism from which they formed. The mantle source of mid-ocean ridge basalts (MORB) has been shown to be quite different and more homogeneous than the mantle source of ocean island basalts (OIB). However, at a global scale, numerous studies revealed that Indian MORBs are isotopically distinct from the Pacific and North Atlantic MORB [*Dupré and Allègre*, 1983; *Hart*, 1984; *Hamelin and Allègre*, 1985; *White et al.*, 1987; *Ito et al.*, 1997]. Indeed, *Dupré and Allègre* [1983] reported that volcanic rocks of the Indian Ocean ridges are variably enriched in Sr and Pb radiogenic isotopes. Such isotopic compositions, found along the Indian and South-Atlantic ridges, are referred as DUPAL anomaly [*Dupré and Allègre*, 1983; *Hart*, 1984].

[3] The plume/ridge interactions can be described by three successive and possible geometries: (1) a ridge approaching a plume, (2) a ridge above a plume, and (3) a ridge moving away from a plume. The latter geometry has long-term consequences on the interaction dynamics as ridge and plume melting zones may remain connected for a long time [*Ito et al.*, 1997; *Ribe and Delattre*, 1998; *Maia et al.*, 2001]. When a ridge is located above a plume, the excess heat results in enhanced melting and longer and more voluminous magmatic production. Such increased magmatic production leads to the construction of an axial plateau comparable to the Azores and Iceland oceanic plateaus (Atlantic Ocean) [*Hart et al.*, 1973; *Schilling*, 1991; *Searle et al.*, 1998; *Cannat et al.*, 1999; *Gente et al.*, 2003]. However, all oceanic plateaus do not result from a plume-ridge interaction. For example, in the Indian Ocean, the Kerguelen plateau has been interpreted as formed from the initial volcanism associated with the Kerguelen mantle plume [*Duncan and Storey*, 1992; *Coffin et al.*, 2002]. The Amsterdam–St. Paul (ASP) system successively underwent the three geometries, which makes it a target of major interest for a global study of plume-ridge interactions.

[4] The MD157/PLURIEL cruise (N/O Marion Dufresne, September/October 2006, P. I.: M. Maia) was dedicated to the mapping and sampling of the plateau and of a chain of seamounts built on the Australian plate, and named the Chain of "Dead Poets" (CDP; Figure 1). The geochronological study resulting from this sampling and the geophysical data have been presented elsewhere [*Courreges*, 2010; *Janin et al.*, 2011; *Maia et al.*, 2011]. These previous studies revealed the complexity of (1) this ridge-hot spot interaction, resulting in a multistage construction of the plateau, and (2) of the regional geodynamics due to the diffuse boundary within the Indo-Australian plate. Observations revealed that the ASP plateau activity was due to two temporally distinct magmatic phases (1) an on-axis stage due to the interaction between ASP hot spot and the Southeast Indian Ridge (SEIR) and leading to the formation of a thick oceanic crust and (2) an off-axis stage allowed the construction of seamounts over the pre-existing plateau. To the northeast, the Chain of Dead Poets (CDP), is parallel to the ASP hot spot modeled track and could be linked to ASP hot spot intraplate activity prior to its interaction with the SEIR. However, *Janin et al.* [2011] revealed a rather complex dynamic. This volcanic chain is composed of two generations of seamounts related to (1) an excess of heat in the mantle caused by ASP plume activity for the oldest events and (2) a later pulse of ASP plume and an erupting process favored by the tectonic consequences of the diffuse divergence between the Capricorn and Australian plates for the younger stage. This work on new dredged samples of both the CDP and ASP plateau samples is related to those previous studies and focuses on the geochemical and isotopic aspects. In this frame, the main goal of this paper is to understand and characterize the sources of the magmatism and their interactions.

2. Geological Settings

[5] The construction of the ASP plateau began about 10 Myr ago [*Maia et al.*, 2008, 2011] and resulted in two separate magmatic stages: on-axis

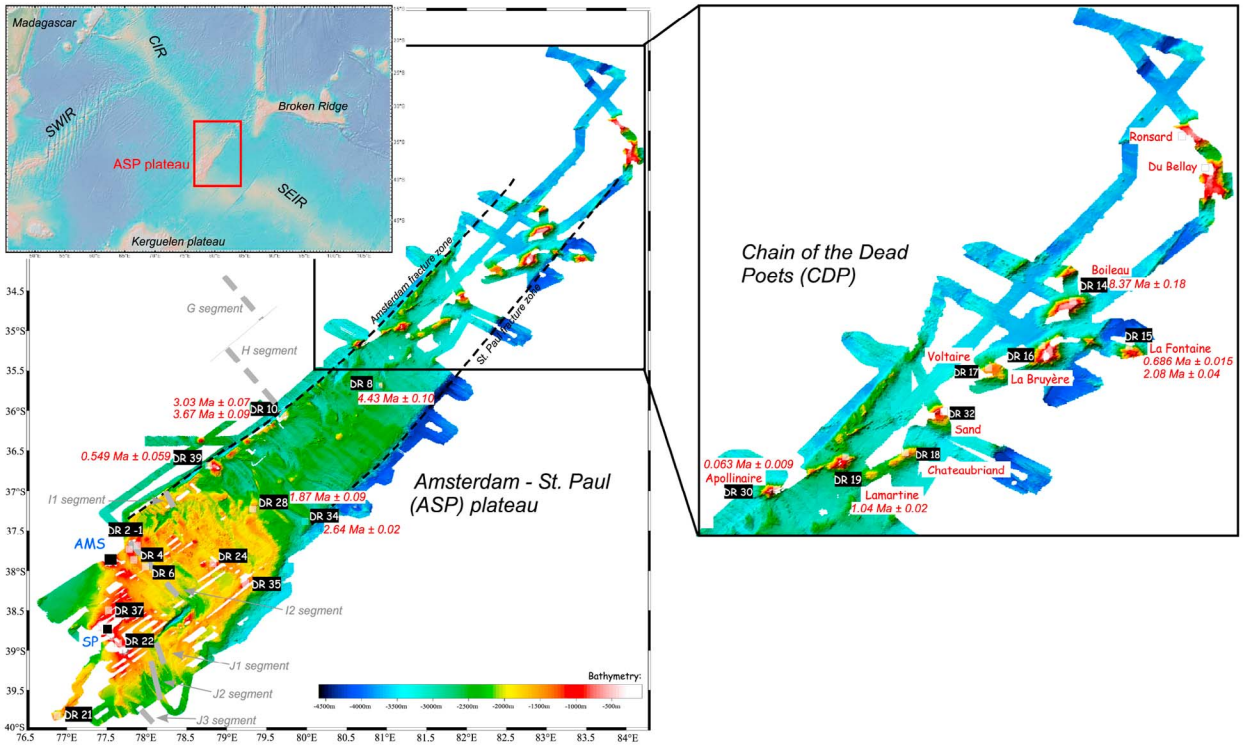

Figure 1. Bathymetry of ASP plateau with a focus on the Chain of Dead Poets mapped during the MD157/PLURIEL cruise (adapted from *Janin et al.* [2011]). White squares (in transparency) represent basaltic samples with the related dredge (PLU DR) number. On the Chain of Dead Poets the name of the seamounts are noted. Two seamounts are named without dredge number because no basalt samples were available. Black squares are the location of Amsterdam (AMS) and St Paul (SP) islands. Dotted lines are the Fracture Zones limiting ASP plateau. Geochronological data are from *Janin et al.* [2011].

and off-axis successively. The difference between on- and off-axis magmatism is highlighted by the morphology of the structure with (1) on-axis magmatism, building a thicker oceanic crust, and (2) off-axis magmatism, occurring later, and resulting into the construction of seamounts on the oceanic floor. The ASP plateau supports Amsterdam and St. Paul islands and several seamounts. Those islands have been the object of early studies [*von Hochstetter*, 1866; *Velain*, 1878; *Reinisch*, 1909]. In the 1970s, *Gunn et al.* [1971], *Watkins and Nougier* [1973], *Watkins et al.* [1974], *Hedge et al.* [1973], and *Watkins et al.* [1975] provided an extensive geological study of the islands and revealed that they were globally less that 0.7 Ma old for Amsterdam and 0.4 Ma old for St. Paul. In addition, recent paleomagnetic and Ar geochronology on the most recent lava flows have produced much younger ages of 26 +/− 15 ka and 18 +/− 9 ka for Amsterdam Island [*Carvallo et al.*, 2003]. *Johnson et al.* [2000] described the seamount Boomerang discovered and mapped during the eponym cruise (R/V Melville, 1996) and located northward of Amsterdam Island, next to the SEIR axis. The presence of fresh hydrothermal sediments and ^{210}Po-^{210}Pb zero age for one seamount basalt provided evidence that Boomerang seamount may be the current active ASP plume location.

[6] Amsterdam and St Paul islands belong to ASP plateau and are located close to 38°30′S and 77°50′E. They and constitute the only emerged part in the vicinity of the SEIR. This plateau, resulting of the interaction between the SEIR and the ASP plume, is located between Amsterdam and St. Paul fracture zones and is crosscut by several SEIR segments (Figure 1), e.g. I1 to J2 segments, according to *Royer and Schlich* [1988].

[7] The SEIR shows a prominent U-shaped shift to the southwest on the plateau and southward (from 77°E to 79°E). This geometry is due to a ridge jump of four segments (J4 to K segment) toward the Kerguelen hot spot (i.e. SW) shortly after the ridge rifted the Kerguelen plateau 40 Myr ago [*Müller*

et al., 1993; *Frey et al.*, 2000]. However, there is no clear evidence so far that the Kerguelen hot spot is still interacting with the SEIR. The geochemical variations revealed by the lavas of the J4 to K segment, when compared to those located northward of the ASP plateau, may simply reflect intrinsic heterogeneities of the Indian upper mantle [*Mahoney et al.*, 2002; *Nicolaysen et al.*, 2007]. It seems thus very unlikely to find some Kerguelen hot spot signature in ASP plateau lavas. *Doucet et al.* [2004] showed that the Amsterdam and St. Paul islands have distinct geochemical characteristics and distinct from the Kerguelen hot spot. In addition, their characteristics are inconsistent with a simple binary mixing between the heterogeneous ambient Indian upper mantle and an ASP plume radiogenic in Pb end-member. These authors then proposed that Amsterdam and St. Paul islands were formed by melts derived from laterally isotopically distinct zones of the ASP plume.

[8] The isotopic compositions of Sr-Nd-Pb-He of the SEIR segments close to ASP plateau reveal the influence of the nearby hot spot [*Graham et al.*, 1999; *Nicolaysen et al.*, 2007]. These authors showed that the heterogeneous isotope ratios of the MORB erupted on the ASP plateau could be modeled by a mixing between the mantle end-member "C" [*Hanan and Graham*, 1996] and DUPAL-like material [*Hart*, 1984]. The DUPAL anomaly is a shift of composition known in the Indian Ocean lavas when compared to Pacific and north Atlantic MORB. The cause of this anomaly, revealed by *Dupré and Allègre* [1983], is still debated today and several models exist in the literature. The different models and our preferred interpretation will be developed in section 6.2.

[9] Literature data belong to the most recent part of the ASP plateau (ridge axis, islands and nearby seamounts [*Graham et al.*, 1999; *Burnard et al.*, 2002; *Doucet et al.*, 2004; *Nicolaysen et al.*, 2007]) whereas the ASP hot spot/SEIR interaction system results from a much longer period of activity of the plateau (presently in the early stage of breakup [*Maia et al.*, 2001]). The Chain of Dead Poets (CDP) may also be due to ASP hot spot activity and has to be taken into account to understand the dynamics of such interaction and its evolution. This work therefore presents the first attempt to describe and model in space and time the evolution of a ridge hot spot/interaction within the surrounding mantle. We will show that ASP plateau lavas results from the mixing of three distinct components: (1) ASP hot spot, (2) the Indian MORB mantle and (3) a lower continental crust component giving the DUPAL flavor to the mixing.

3. Samples

[10] The sample set is composed of both on- and off-axis samples (Figure 1). The off-axis samples come either from the plateau itself or from identified seamounts. The on-axis magmatic stage, responsible for the construction of the plateau is represented by three samples: PLU DR 6-1-1, PLU DR 6-2-2 and PLU DR 34-1-1. The northeastern part of the plateau, located on the Australian plate, supports a volumetrically limited volcanic chain of seamounts, which shows a variety of morphologies ranging from small volcanoes (PLU DR 10-1-1, PLU DR 10-2-2) to large seamounts (PLU DR 39-1-1/ Rimbaud). They were either built onto the plateau or on its edge and represent a later off-axis magmatic stage [*Janin et al.*, 2011].

[11] The seamount Chain of the Dead Poets (CDP) lies northeastward of the ASP plateau and consists in two groups of seamounts: (1) two 8–10 Ma old large flat-topped seamounts, and (2) six smaller conical seamounts formed during the last 2 Myr. Those eight seamounts are, from SW to NE, Apollinaire, Lamartine, Chateaubriand, Sand, Voltaire, La Bruyère, Boileau and La Fontaine (Figure 1). Boileau and La Bruyère seamounts, which are related to the first stage of activity of ASP plume on the Australian plate, are two to four times bigger than the others. Insufficient bathymetric data northeastward, in the vicinity of Ronsard and Du Bellay seamounts, do not allow us to confidently relate these edifices to this early phase of volcanism. However, taking into account their position at the northeastern tip of the CDP tip, we consider them as part of this alignment.

4. Methodology

[12] Some of the samples have been exposed to seawater for some Myr. Therefore, only the freshest samples were chosen for geochemical investigations after macroscopic and microscopic observation. Weathered parts, such as altered rims and/or filled vesicles were mechanically removed. Then, the samples were powdered in an agate grinder and prepared following the required chemical protocols. When possible, we also performed analyses on glass chips. K-Ar datings on rocks of these samples have been presented elsewhere [*Janin et al.*, 2011]. The main samples have been described in *Janin*

et al. [2011] and do not exhibit major evidence of secondary mineralization. Some alteration phases were clearly aggregated in a small area for the oldest samples, and have been mechanically removed. The L. O. I. (Loss on Ignition) of the samples is generally lower than 1.5%. Consequently we are confident in excluding post-eruption modification of the sample compositions.

4.1. Analyses of Major and Trace Elements

[13] The bulk rock major elements were analyzed by Inductively Coupled Plasma Atomic Emission Spectrometer (ICP AES) Horiba Jobin Yvon Ultima 2 (PSO/IUEM, Plouzané, France), following the protocol adapted from *Cotten et al.* [1995]. Each powdered sample was digested in Teflon vials within HF 32N and HNO_3 14.4N and the dry residue was dissolved in a H_3BO_3 solution. PMS, BELC and ACE internationals standards were used as internal and external control. The precision of measurements performed on that instrument is usually better than 1% for both SiO_2 and TiO_2, 2% for Al_2O_3 and Fe_2O_3, and better than 4% for the other major oxides. In our case, replication of measurements gives relative standard deviation better than 1.5% for all the elements.

[14] Trace element concentrations were determined using a High Resolution Inductively Coupled Plasma Mass Spectrometer (HR ICP-MS) Thermo Finnigan Element II (PSO/IUEM, Plouzané, France), following a method adapted from *Barrat et al.* [2007]. About 100 mg of sample were digested in Teflon vials within distilled HF 32N and HNO_3 14.4N. The dry residue was dissolved in HNO_3 14.4N and then in HCl 3N. An aliquot of the solution was diluted in HNO_3 0,3N and spiked with Tm spike. BCR2 and BIR1 were used as external control and BHVO-2 was used for internal control. The precision of measurements was better than 5% for all elements.

4.2. Radiogenic Isotopes

[15] Prior to the chemical separation all powders of submarine samples were leached by adding 4 ml of 6N HCl and kept at 85°C for a period of 20 to 40 min. The leached samples were rinsed thrice with de-ionized water to eliminate potential seawater contamination.

[16] Hf and Pb isotopes were measured on a Thermo Fischer Neptune MC-ICP-MS (PSO/Ifremer, Plouzané, France). For Hf separation each sample powder was dissolved with a HF -HNO_3 3:1 mixture at 85°C for 48 h and evaporated to dryness. Hf of the dry residue followed the procedure of *Blichert-Toft et al.* [1997]. JMC 475 standard was used for internal control (mean value (n = 17) $^{176}Hf/^{177}Hf = 0.282154 \pm 0.000013$ (2σ)/recommended value $^{176}Hf/^{177}Hf = 0.282163$). Blanks were less than 50 pg.

[17] For Pb separation, samples were dissolved with a HF-HBr 3:1 (Romil-UpA™ - [Pb < 1 ppt]) mixture for 48 h and then evaporated to dryness. Chemical chromatography was performed on anionic AG1X8 200–400 mesh columns following the procedure of *Manhes et al.* [1978]. The Pb fraction was purified a second time on the same column. The non-retained fraction was kept for Sr and REE separation. Later, the Pb fraction was dissolved in HNO_3 2% and spiked with Tl prior to analysis. NIST 981 standard was used for internal control (mean values (n = 36) $^{206}Pb/^{204}Pb = 16.931 \pm 0.006$ (2σ); $^{207}Pb/^{204}Pb = 15.488 \pm 0.005$ (2σ); $^{208}Pb/^{204}Pb = 36.692 \pm 0.014$ (2σ)/recommended values $^{206}Pb/^{204}Pb = 16.937 \pm 0.006$; $^{207}Pb/^{204}Pb = 15.491 \pm 0.008$; $^{208}Pb/^{204}Pb = 36.721 \pm 0.016$). Blanks were less than 100 pg.

[18] Sr and Nd isotopes were determined on a Thermo Electron™ Triton T1 (PSO/IUEM, Plouzané, France) using procedures adapted from *White and Patchett* [1984] and *Richard et al.* [1976]. Fractions eluted from the Pb protocol were evaporated to dryness then re-dissolved twice in HNO_3 14N and dried again. The Sr separation on ion exchange resin was performed on cationic AG50X8 columns. Sr fractions of highly alkaline samples were purified a second time. REE were eluted from the same solution. Nd was then separated using LnSpec Eichrom resin. Sr isotopes determinations were run on a single W filament coated with Ta activator [*Birck*, 1986]. NBS 987 was used for internal control (mean value (n = 31) $^{87}Sr/^{86}Sr = 0.710262 \pm 0.000016$ (2σ)/recommended value $^{87}Sr/^{86}Sr = 0.710248$). Blanks were less than 600 pg. Nd isotopes determinations were run on Re double filament. La Jolla standard was used for internal control (mean value (n = 16) $^{144}Nd/^{143}Nd = 0.511845 \pm 0.000017$ (2σ)/recommended value $^{144}Nd/^{143}Nd = 0.511850$). Blanks were less than 400 pg.

5. Results

[19] Major and trace elements, and isotope compositions are presented in Tables 1 and 2.

Table 1 (Sample). Major and Trace Element Concentrations of ASP Plateau and CDP Samples[a] [The full Table 1 is available in the HTML version of this article]

	Sample									
	PLU DR1-2-4	PLU DR1-2-5	PLU DR2-1-1	PLU DR4-1-3	PLU DR4-1-5	PLU DR6-1-1	PLU DR6-2-2	PLU DR8-1-1	PLU DR10-1-1	PLU DR10-2-2
Location	Boomerang	Boomerang				SEIR	SEIR			
Latitude	S37°41.53	S37°41.53	S37°35.67	S37°51.80	S37°51.80	S38°04.08	S38°04.08	S35°40.70	S36°03.69	S36°03.69
Longitude	E77°53.91	E77°53.91	E78°00.40	E78°03.00	E78°03.00	E78°12.23	E78°12.23	E80°55.10	E79°41.77	E79°41.77
SiO_2	49.51	50.01	50.27	50.19	50.66	54.90	53.72	47.20	48.48	48.23
TiO_2	2.50	2.50	1.98	2.23	1.92	1.81	1.92	1.87	1.48	1.45
Al_2O_3	13.81	13.67	14.12	13.88	14.38	13.55	13.59	15.50	14.65	15.39
Fe_2O_3	14.26	14.14	12.91	13.26	12.09	12.05	12.18	10.93	12.53	12.12
MnO	0.22	0.22	0.20	0.21	0.19	0.20	0.19	0.15	0.22	0.33
MgO	4.99	4.71	5.52	5.54	5.96	2.80	3.36	5.73	6.07	5.86
CaO	9.02	9.07	10.34	9.42	10.21	6.39	6.90	12.33	11.93	12.17
Na_2O	3.37	3.37	2.95	3.09	2.76	3.90	3.70	2.65	2.68	2.66
K_2O	0.63	0.67	0.60	0.71	0.66	1.28	1.17	0.42	0.44	0.37
P_2O_5	0.29	0.29	0.23	0.29	0.28	0.46	0.37	0.32	0.25	0.22
Total	98.60	98.66	99.12	98.82	99.10	97.34	97.09	97.10	98.71	98.79
Cs	0.193	0.191	0.237	0.203	0.196	0.458	0.410	0.150	0.449	0.313
Rb	12.8	8.98	10.5	15.5	12.6	30.6	36.0	4.77	8.81	7.87
Ba	151	94.6	101	145	129	271	256	70.6	34.3	35.7
Th	2.61	1.44	1.53	2.26	2.41	5.57	4.37	1.72	0.963	0.809
U	0.565	0.345	0.353	0.543	0.553	1.13	0.990	0.506	0.231	0.279
Nb	29.1	17.1	14.8	26.4	24.9	46.4	40.5	18.5	8.86	7.82
Ta	1.85	1.04	0.852	1.58	1.52	2.77	2.31	1.20	0.541	0.481
La	19.7	12.1	12.3	18.5	17.0	35.3	32.9	13.2	7.71	7.97
Ce	43.4	26.8	28.0	40.4	37.7	76.0	71.1	26.8	17.6	19.1
Pr	5.65	3.48	3.73	5.16	4.86	9.54	8.93	3.97	2.57	2.51
Pb	1.51	0.910	1.08	1.34	1.31	2.52	2.38	1.74	1.73	9.87
Nd	24.1	15.2	17.1	22.3	21.1	39.8	37.3	18.0	12.2	11.9
Sr	310	193	237	248	216	201	212	277	175	169
Sm	6.00	3.78	4.52	5.56	5.20	9.38	8.81	4.67	3.52	3.45
Zr	230	118	169	180	208	456	363	166	123	91.5
Hf	5.01	2.66	3.84	4.12	4.65	9.66	7.77	3.89	2.91	2.27
Eu	2.06	1.30	1.58	1.84	1.70	2.67	2.56	1.64	1.29	1.27
Gd	6.84	4.33	5.38	6.36	6.04	10.5	9.97	5.34	4.52	4.47
Tb	1.10	0.695	0.876	1.04	0.982	1.70	1.65	0.848	0.797	0.773
Dy	6.67	4.29	5.47	6.40	6.02	10.5	9.99	5.08	5.06	4.92
Ho	1.37	0.896	1.13	1.34	1.26	2.19	2.11	1.03	1.08	1.07
Er	3.78	2.42	3.1	3.71	3.49	6.15	6.05	2.73	3.07	3.03
Y	40.0	39.8	32.4	38.8	35.8	63.6	63.3	32.1	32.3	31.1
Yb	3.32	2.21	2.82	3.34	3.20	5.66	5.50	2.35	2.83	2.72
Lu	0.476	0.321	0.404	0.485	0.460	0.827	0.808	0.332	0.411	0.404

[a]Symbol g = glass samples. The major elements concentrations are given in wt%. The trace elements concentrations are given ppm.

Table 2. Isotopic Compositions of ASP Plateau and CDP Samples[a]

	$^{87}Sr/^{86}Sr$	2σ	$^{143}Nd/^{144}Nd$	2σ	$^{206}Pb/^{204}Pb$	2σ	$^{207}Pb/^{204}Pb$	2σ	$^{208}Pb/^{204}Pb$	2σ	$^{176}Hf/^{177}Hf$	2σ
PLU DR 1-2-2 g	0.704117	0.000010	0.512833	0.000001	18.814	0.001	15.590	0.001	39.031	0.003	0.283070	0.000005
PLU DR 1-2-4					19.124	0.001	15.616	0.001	39.432	0.003	0.283068	0.000005
PLU DR 2 T-g					19.101	0.001	15.600	0.001	39.441	0.003		
PLU DR 2-1-1 S-g	0.704300	0.000010			18.583	0.001	15.582	0.001	38.975	0.003		
PLU DR 2-1-1	0.704213	0.000008	0.512766	0.000006	18.578	0.001	15.585	0.001	38.971	0.002	0.282973	0.000006
PLU DR 2-1-2 g	0.704134	0.000008	0.512776	0.000006	18.579	0.001	15.585	0.001	38.971	0.003		
PLU DR 4-1-3	0.703842	0.000006	0.512838	0.000006	19.134	0.001	15.617	0.001	39.496	0.003	0.283056	0.000006
PLU DR 4-1-4 g	0.703947	0.000011	0.512828	0.000014	18.856	0.001	15.587	0.001	39.262	0.003		
PLU DR 6 g	0.703940	0.000008	0.512819	0.000006	18.854	0.001	15.589	0.001	39.271	0.003		
PLU DR 6-1-1	0.703935	0.000008	0.512814	0.000008	18.849	0.001	15.584	0.001	39.251	0.003	0.283047	0.000007
PLU DR 6-1-2 g	0.703935	0.000007	0.512810	0.000006	18.843	0.001	15.580	0.001	39.234	0.002		
PLU DR 6-1-3 g					18.851	0.001	15.585	0.001	39.258	0.003		
PLU DR 6-2-1 g					18.829	0.002	15.582	0.001	39.227	0.004		
PLU DR 6-2-2					18.838	0.001	15.583	0.001	39.236	0.003	0.283038	0.000005
PLU DR 8-1-1	0.703983	0.000008	0.512846	0.000008	18.962	0.001	15.621	0.001	39.134	0.003	0.283051	0.000005
PLU DR 10-1-1					18.839	0.001	15.577	0.001	38.961	0.003	0.283127	0.000006
PLU DR 10-1-1 g	0.703644	0.000008			18.819	0.002	15.645	0.001	38.934	0.004		
PLU DR 10-2-2	0.703926	0.000006	0.512876	0.000008	18.786	0.001	15.658	0.001	38.868	0.003	0.283137	0.000007
PLU DR 14-1-1	0.704008	0.000009	0.512785	0.000004	18.958	0.001	15.593	0.001	39.174	0.003	0.282994	0.000007
PLU DR 15-1-1	0.704090	0.000008	0.512838	0.000006	19.012	0.001	15.640	0.001	39.132	0.002	0.283006	0.000005
PLU DR 15-2-3	0.703864	0.000006	0.512849		19.134	0.001	15.611	0.001	39.333	0.003	0.282989	0.000007
PLU DR 15-3-2	0.703905	0.000006	0.512849	0.000006	19.230	0.001	15.621	0.001	39.426	0.003	0.282997	0.000005
PLU DR 16-3-2	0.704123	0.000006	0.512836	0.000008	19.123	0.001	15.604	0.001	39.348	0.004	0.282986	0.000005
PLU DR 19-2-2	0.703838	0.000008	0.512824	0.000008	18.835	0.001	15.581	0.001	39.233	0.003	0.283010	0.000007
PLU DR 21	0.703967	0.000008	0.512818	0.000006	18.747	0.002	15.631	0.002	38.795	0.004	0.283090	0.000005
PLU DR 22-1-1					18.671	0.001	15.596	0.001	38.977	0.002	0.283044	0.000006
PLU DR 22-3-1 g	0.704107	0.000006	0.512837	0.000006	18.629	0.001	15.567	0.001	38.920	0.003	0.283043	0.000006
PLU DR 22-7-1 g	0.704134	0.000008	0.512839	0.000006	18.636	0.002	15.574	0.002	38.940	0.004		
PLU DR 24-1	0.705451	0.000006	0.512464	0.000008	17.384	0.003	15.571	0.002	38.121	0.006	0.282723	0.000005
PLU DR 24-1-4 g	0.705451	0.000008	0.512483	0.000016	17.487	0.001	15.583	0.001	38.196	0.003		
PLU DR 24-1-4X-g	0.705304	0.000006	0.512478	0.000006	17.375	0.004	15.566	0.004	38.074	0.010	0.282645	0.000006
PLU DR 28-1-1	0.703630	0.000008	0.512932	0.000008	18.667	0.001	15.624	0.001	38.809	0.004	0.283209	0.000006
PLU DR 30-1-1	0.703870	0.000008	0.512809	0.000010	19.617	0.001	15.664	0.001	39.892	0.003	0.282978	0.000005
PLU DR 30-2-1	0.703938	0.000008	0.512817	0.000006	19.490	0.001	15.670	0.001	39.741	0.003	0.282991	0.000006
PLU DR 32-1	0.704192	0.000008	0.512819	0.000010	18.625	0.002	15.615	0.002	38.707	0.005	0.282992	0.000007
PLU DR 34-1-1	0.703849	0.000006	0.512878	0.000010	18.523	0.001	15.601	0.001	38.599	0.003	0.283119	0.000006
PLU DR 34-1-1 g	0.703525	0.000008	0.5129	0.000006	18.613	0.001	15.541	0.001	38.806	0.004		
PLU DR 35-1-1	0.704271	0.000006	0.512748	0.000008	18.704	0.001	15.627	0.001	39.182	0.003	0.283022	0.000006
PLU DR 37-2	0.703873	0.000006	0.512851	0.000006	19.094	0.001	15.628	0.001	39.496	0.003	0.283113	0.000008
PLU DR 39-1-1	0.703760	0.000008	0.512940	0.000008	18.513	0.001	15.615	0.001	38.665	0.004	0.283191	0.000006

[a]Hf and Pb data were performed on Thermo Fischer Neptune MC-ICP-MS (PSO/Ifremer, Plouzané, France). Sr and Nd data were performed on a Thermo Electron™ Triton T1 (PSO/IUEM, Plouzané, France). Replicated and duplicated data are not presented here but revealed the good repeatability of procedures and measurements.

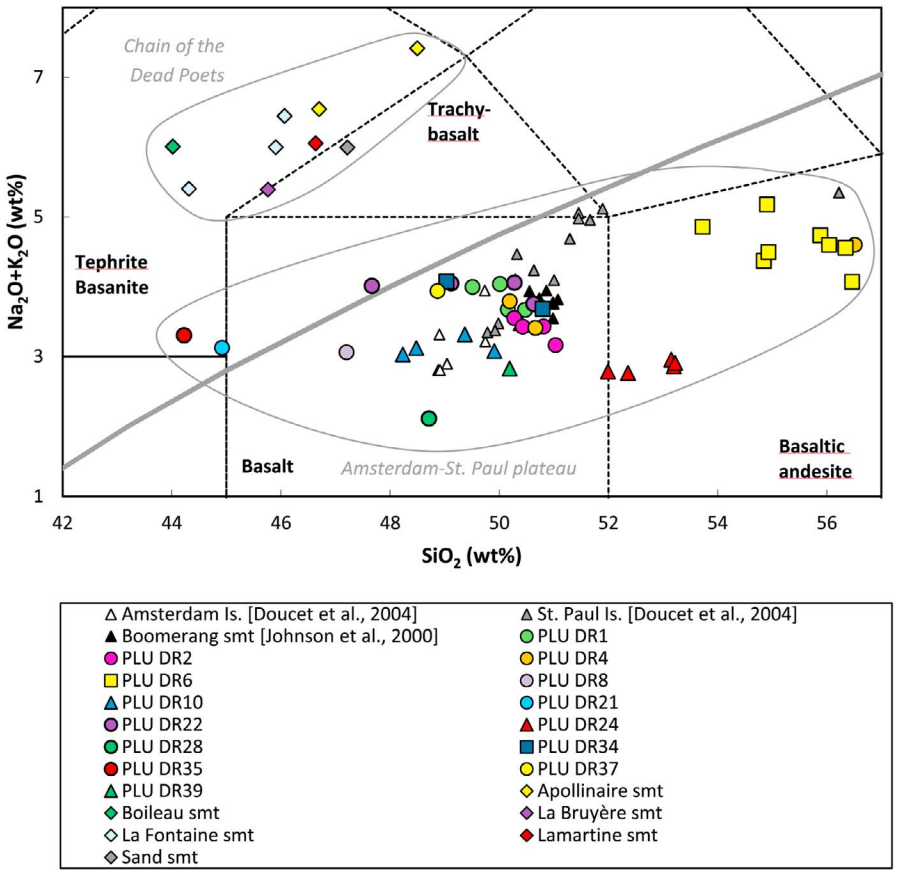

Figure 2. Alkalis versus silica diagram (wt%) illustrating the range of petrological compositions for samples from the Chain of Dead Poets (diamond symbol) and the ASP plateau. On ASP plateau, on-axis magmatism is symbolized by squares. The fields used are from *Le Bas et al.* [1992]. The black line separates alkaline fields from tholeiitic fields. Data from *Johnson et al.* [2000] and *Doucet et al.* [2004] are plotted for comparison. 2σ error bars are smaller than symbol size.

5.1. Major Elements

[20] The SiO_2 contents range between 44% and 56 wt% for 3% < MgO < 8%. A plot of total alkalis versus silica (TAS diagram [*Le Bas et al.*, 1992]; Figure 2) reveals that the plateau samples are mostly tholeiitic while the samples from the CDP are highly alkaline, with a tephrite or basanite composition. Some samples from ASP plateau, precisely from St. Paul Island [*Doucet et al.*, 2004], have a mildly alkaline to transitional composition. Our plateau samples are similar to those of Boomerang seamount [*Johnson et al.*, 2000] and Amsterdam and St. Paul Island [*Doucet et al.*, 2004]. However, the new data set display a larger range in compositions from alkaline primitive lavas to typical N-MORB.

[21] In the CDP samples, the alkalis contents range between 6% and 7.42% and co-vary with SiO_2 within one seamount, which suggests an influence of fractional crystallization processes. At a given Mg# value, the CDP samples are systematically enriched in Al_2O_3, Na_2O, K_2O and P_2O_5, and depleted in SiO_2, when compared to ASP plateau samples. This implies that the samples of the seamount chain have common characteristics, and a common source, despite the temporal dispersion evidenced by *Janin et al.* [2011]. The enrichment of the seamounts is particularly striking in K_2O with contents higher than 1.5% and reaching 2.2%. On the plateau, the maximum K_2O concentration reaches 1.3% for one sample from the current SEIR but the published values typically range between 0.1% and 1% [*Girod et al.*, 1971; *Gunn et al.*, 1971, 1975; *Doucet et al.*, 2004].

5.2. Trace Elements

[22] The trace elements compositions of the samples are plotted in primitive mantle – normalized spidergrams (Figure 3). The CDP and ASP plateau

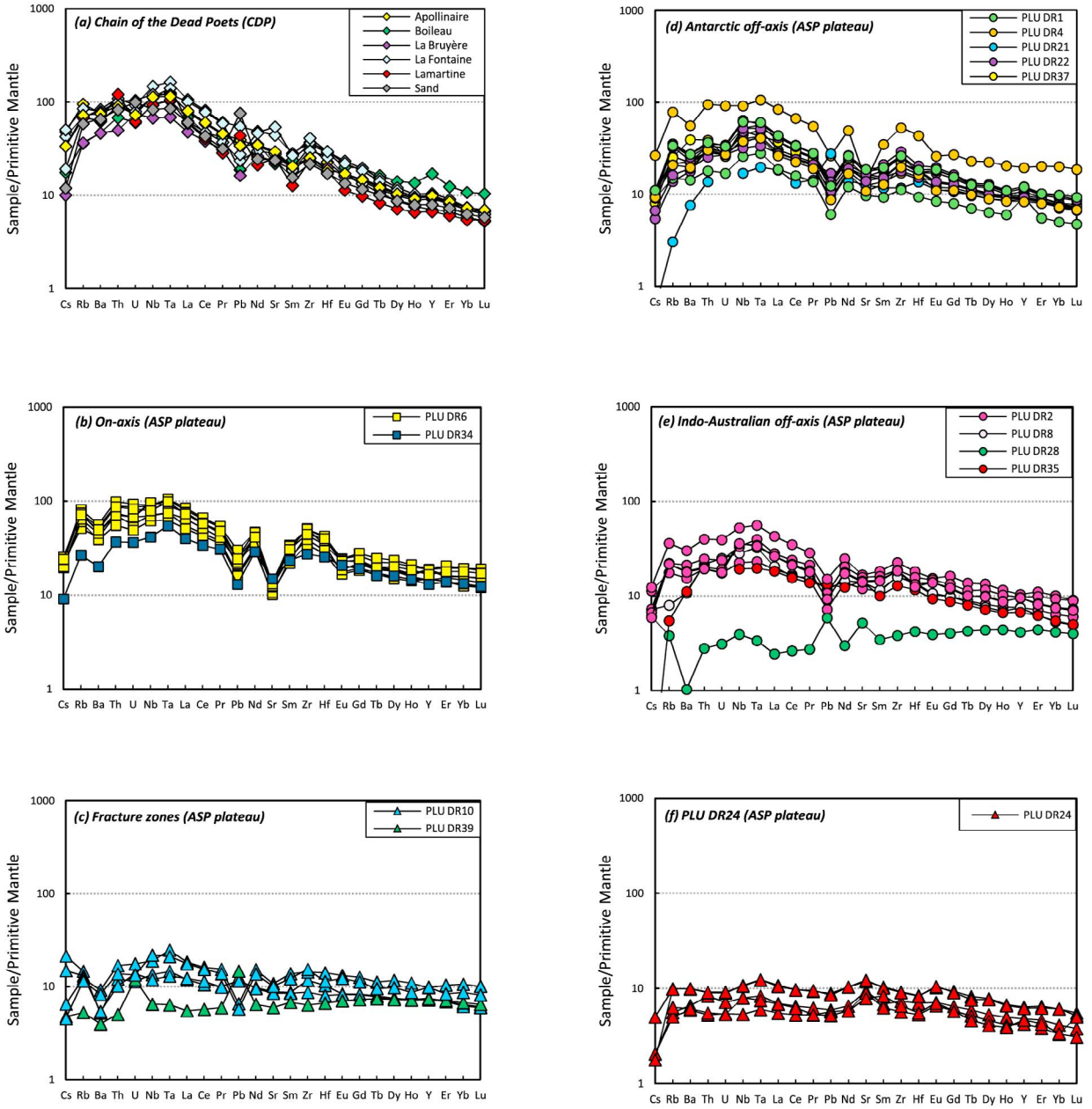

Figure 3. Trace elements patterns of (a) CDP and (b–f) ASP plateau samples normalized to primitive mantle [*McDonough and Sun*, 1995]. To facilitate the reading, samples were plotted according to their geodynamical context. The CDP samples are on the same diagram while ASP plateau samples are divided into off- axis, on-axis and fracture zones magmatism. PLU DR24 samples were separated because of a peculiar isotopic signature discussed in the next paragraph. 2σ error bars are smaller than symbol size.

samples exhibit a wide range of contents. To ease the reading we decided to present separate diagrams, according to their geodynamical context.

[23] The CDP samples exhibits similar patterns with low Cs and HREE contents compared to LREE. In addition, Boileau and La Bruyere seamounts have lower contents in incompatible elements which could be related to a higher degree of partial melting. Surprisingly for oceanic lavas, Lamartine and Sand seamounts exhibit an enrichment in Pb (Pb/Ce > 0,1) but we exclude any possible contamination of the samples because those two seamounts also exhibit enrichment in U and Sr, and in Sr respectively, which could be related to the involvement of a

continental component. This will be discussed later in section 6.2.2.

[24] On ASP plateau, PLU DR6 and PLU DR34 samples represent, respectively, the expression of current and ancient magmatism at the SEIR axis. All the samples exhibit similar patterns suggesting a similar partial melting and/or mantle source. PLU DR 1, 2, 4, 8 and 37 samples are related to off-axis magmatism and have close trace elements contents to those of on-axis magmatism. There is no major difference between on- and off- axis magmatism in terms of trace elements contents (except a small depletion in Sr and Eu for off-axis samples) which suggests similar melting processes. The samples exhibit a negative anomaly in Ba, Pb and Sr. The other off-axis magmatism samples have peculiar compositions. PLU DR21 and PLU DR35 are indeed characterized by low contents in incompatible elements and positive anomalies in U and Pb. PLU DR24 have small, but significant positive anomalies in Ta, Sr and Eu. PLU DR28 is a peculiar sample since it exhibits a typical N-MORB composition. This sample is also characterized by a negative anomaly in Ba and positive anomalies in Cs, Pb et Sr. The samples coming from fracture zones appear relatively heterogeneous but all of them exhibit almost flat trace elements patterns. In addition, PLU DR39 is characterized by positive anomalies in U and Pb, while PLU DR10 samples always exhibit a negative anomaly in Ba and a variable anomaly in Pb.

5.3. Isotope Ratios

[25] Whatever the isotopic ratios used, the samples from ASP plateau and from the CDP do not fall in a homogeneous field. $^{87}Sr/^{86}Sr$ ranges from 0.703525 to 0.705451, $^{143}Nd/^{144}Nd$ from 0.512464 to 0.512975, $^{206}Pb/^{204}Pb$ from 17.375 to 19.617, $^{207}Pb/^{204}Pb$ from 15.532 to 15.658, $^{208}Pb/^{204}Pb$ from 38.121 to 39.892 and $^{176}Hf/^{177}Hf$ from 0.282645 to 0.283209 (Figure 4). However, our results are consistent with previous studies since Amsterdam and St Paul islands' data [*Doucet et al.*, 2004] systematically fall in the field defined by our extreme data.

[26] On the $^{87}Sr/^{86}Sr$ versus $^{143}Nd/^{144}Nd$ diagram (Figure 4), all the samples, including the CDP samples, lay on a trend between the typical Indian MORB DM source and PLU DR24 samples. A simple binary mixing could explain all the observed composition but if so, ASP hot spot cannot be one of its end-members since the CDP exhibits an intermediate composition in such trend. Anyway, the $^{176}Hf/^{177}Hf$ versus $^{206}Pb/^{204}Pb$ diagram (Figure 4) excludes a simple binary mixing since ASP plateau samples fall between the MORB DM and the CDP samples. The extreme CDP compositions are given by the Apollinaire seamounts in terms of $^{206}Pb/^{204}Pb$ but the CDP samples are homogeneous in $^{176}Hf/^{177}Hf$. Again, PLU DR24 samples seem to be an extreme component with a very low $^{176}Hf/^{177}Hf$. Among others, PLU DR2 samples seem to be shifted toward PLU DR24 extreme composition. Such trends are more clearly evidenced in the Pb isotopic space.

[27] On the $^{208}Pb/^{204}Pb$ versus $^{206}Pb/^{204}Pb$ diagram (Figures 4 and 5) the CDP samples lie on a trend between the Indian MORB DM source and the most radiogenic component, measured in the Apollinaire samples, which would thus represent an extreme hot spot signature. All the other samples (CDP + plateau) are distributed toward less radiogenic Pb isotopes. However, they do not fall on the single line trend but display some funnel shaped trend. This trend points toward two less radiogenic components namely (1) the Indian DM (represented by a large number of Indian MORB) and (2) the composition of PLU DR24). In other words, in the Pb isotopic space, the samples are distributed in a triangle having as summits Apollinaire seamount, PLU DR24 and the Indian DM.

6. Discussion

[28] The results presented in the previous section indicate that the origin of ASP plateau lavas is geochemically complex. Our goal here is to discriminate the different components and their origin, in the frame of the "mantle zoo" [*Stracke et al.*, 2005], i.e. C component, HIMU, and EM end-members. The C component, as defined by *Hanan and Graham* [1996], is the common component to every hot spot and corresponds to the lower and primitive mantle. This primitive composition is influenced by several end-members leading to the complexity of OIB signatures. Those end-members are related to recycled material with various origins like (1) HIMU (high $\mu = {}^{238}U/{}^{204}Pb$ ratio), associated to recycled oceanic crust, (2) EM1 (Enriched Material), related to old pelagic sediments, recycled continental lithosphere, … and (3) EM2, related to recycled detritical sediments, metasomatized lithosphere, …

[29] In the following paragraph, we will first constrain the composition and origin the ASP hot spot

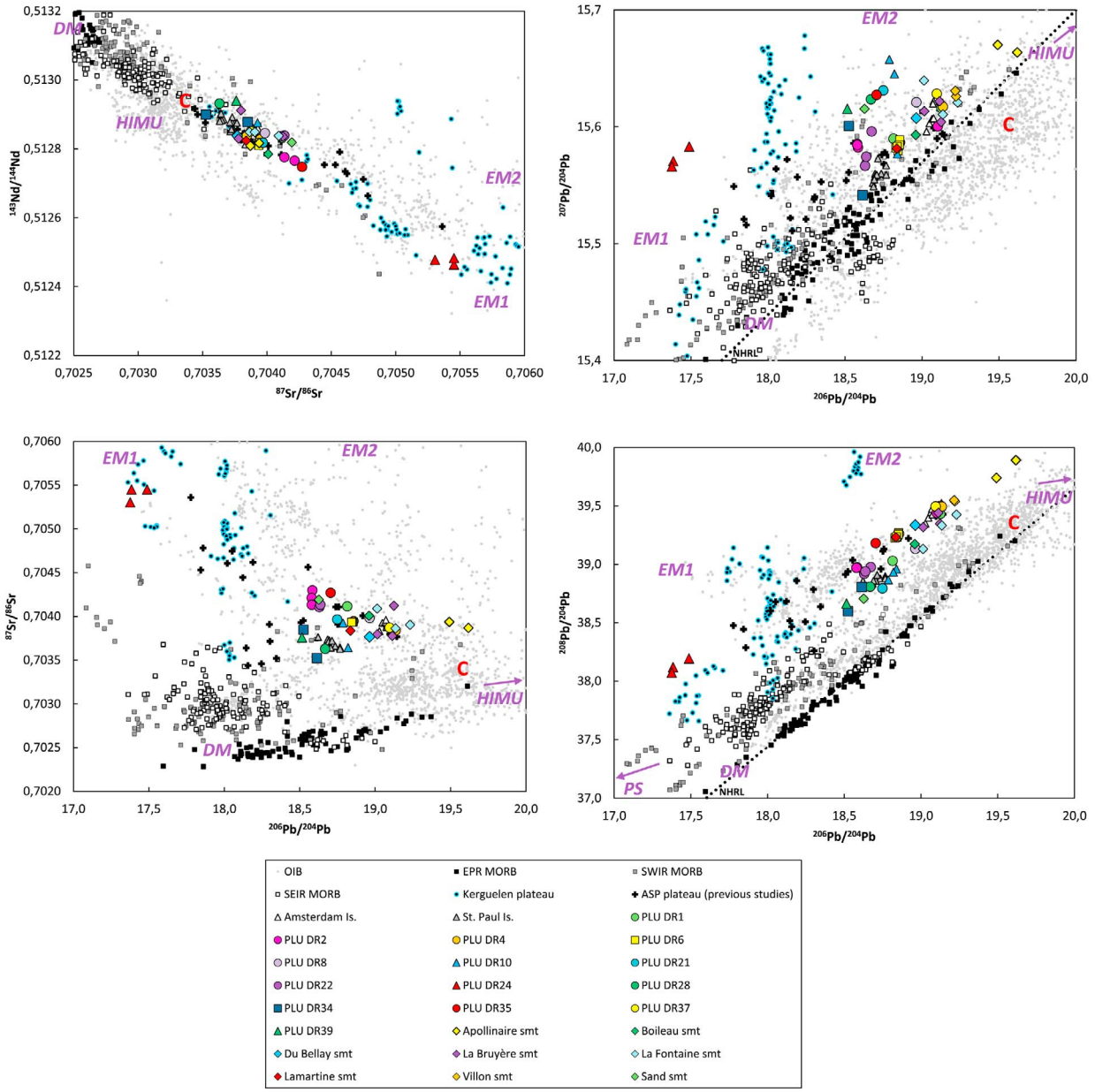

Figure 4. Sr-Nd-Pb-Hf isotope ratios of CDP (diamond symbols) ASP plateau (all other symbols) samples. We added for comparison the global OIB values (gray circle), the SEIR, SWIR and EPR values (respectively white, gray and black squares) (compiled files from the GEOROC database available at http://georoc.mpch-mainz.gwdg.de/georoc/), and the literature data on ASP plateau [*Dosso et al.*, 1988; *Graham et al.*, 1999; *Johnson et al.*, 2000], and Amsterdam and St. Paul Islands [*Doucet et al.*, 2004], and Kerguelen plateau. The literature data on ASP plateau include data coming from the SEIR segments crossing ASP plateau. 2σ error bars are smaller than symbol size. All isotopic components discussed in the text are shown on the diagrams (C = common component from *Hanan and Graham* [1996], DM = Depleted Mantle, EMs = Enriched mantle, HIMU = high $^{238}U/^{204}Pb$ ratio – see text for discussion), as well as pelagic sediments (PS) As in Figures 2 and 3, similar symbols means similar geodynamical context (see text for details). The color code is related to the relative enrichment in $^{208}Pb/^{204}Pb$ in the $^{208}Pb/^{204}Pb$ versus $^{206}Pb/^{204}Pb$ diagram. Samples from the ASP-DM trend are represented with cold colors while samples from the ASP-DR24 trend are symbolized with hot colors.

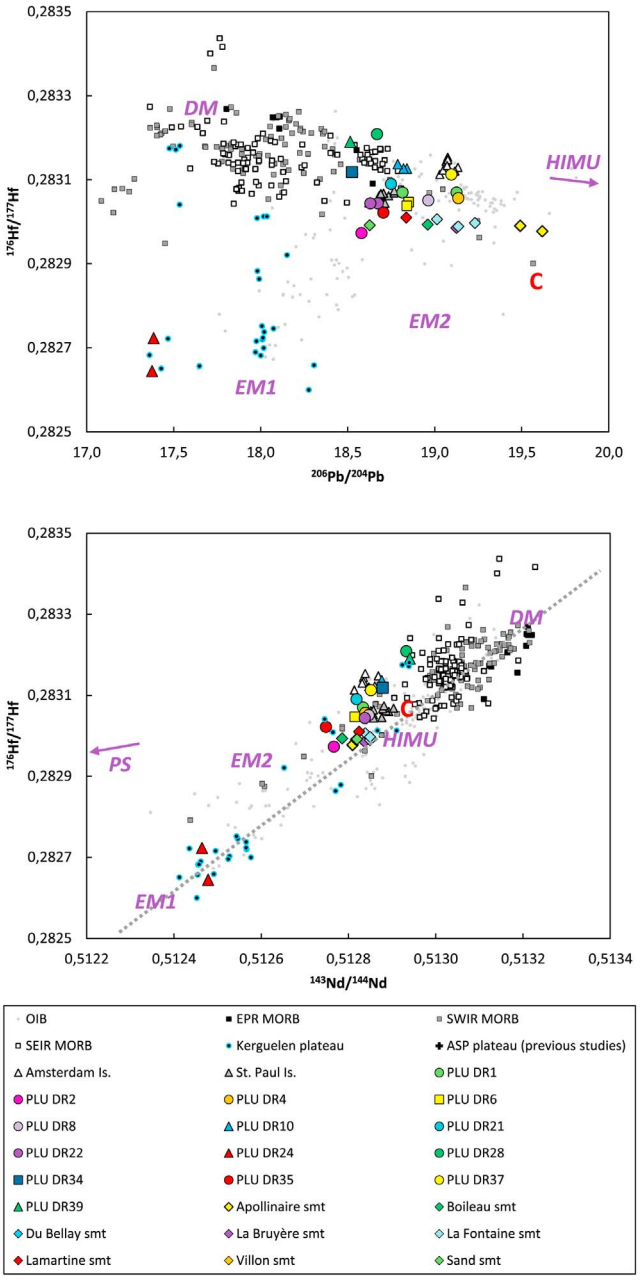

Figure 4. (continued)

itself through these possible end-members. Then, in the second, we will focus on the influence of the DUPAL anomaly on ASP plateau lavas, and we will constrain its origin regarding this new data set.

6.1. Chain of the Dead Poets, an Extreme Hot Spot Component

[30] As shown earlier, the Pb isotopic diagrams (Figure 4) seem to be the most discriminating so the Pb isotopes will be principally used in the discussion. Other isotopic and trace elements constraints will be considered when necessary to strengthen the demonstration.

6.1.1. Pb-Pb Systematic and Plume-Ridge Interaction

[31] Linear Pb-Pb isotopes correlations can be interpreted either as isochrons or as binary mixing

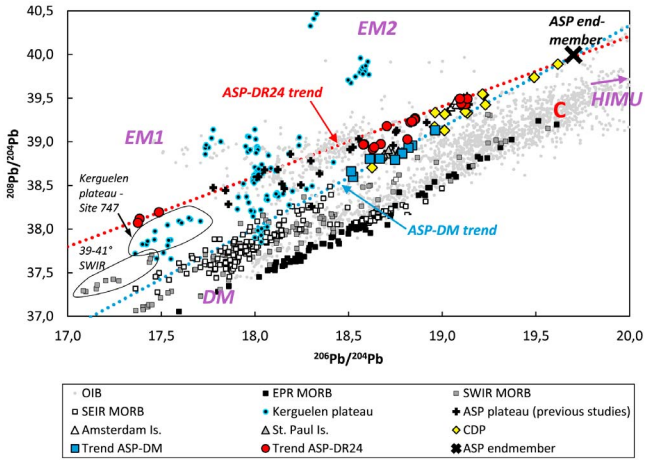

Figure 5. ASP-DM trend and ASP-DR24 trend (see text for details) determined by regression lines through the extreme data (respectively blue and red dotted lines). Since ASP plume influence is involved in both trends the most likely Pb composition of ASP end-member in represented by the intercept of both lines: $^{206}Pb/^{204}Pb$ = 19.7 and $^{208}Pb/^{204}Pb$ = 40.

lines [*Tatsumoto*, 1978; *Abouchami et al.*, 2000]. In Figure 4, the straight line delineated by most of the CDP samples would define a 5 Ga isochron, which, regarding the age of the Earth, allows to rule out any chronological correlation. Therefore, given the geodynamical context, this line will be regarded as a mixing line in the frame ridge-hot spot interaction in the following discussion.

[32] As evoked earlier in section 5.3, the triangular shape defined by the data set in the Pb isotopic space requires at least three distinct components to account for the isotopic variations of ASP lavas. All but two (Boileau and Lamartine seamounts) CDP samples lie on a single mixing line between a rather radiogenic Pb component ($^{206}Pb/^{204}Pb$ = 19.6) and the Indian DMM as defined elsewhere [*Dupré and Allègre*, 1983; *Hart*, 1984; *Mahoney et al.*, 1992; *Rekhämper and Hofmann*, 1997; *Chauvel and Blichert-Toft*, 2001; *Hanan et al.*, 2004]. The CDP samples are characterized by a higher $^{87}Sr/^{86}Sr$ and $^{208}Pb/^{204}Pb$ for a given $^{206}Pb/^{204}Pb$ and their dispersion along this trend reflects either an intrinsic heterogeneity of the mantle plume, or a mixing with the surrounding upper mantle. The first case is rather unlikely as it requires a highly depleted component in the plume, similar to the Indian MORB mantle. The first seamount generation of the CDP (Boileau and La Bruyère >8 Ma [*Janin et al.*, 2011]), which belongs to ASP plume intraplate activity, lies on this mixing line but do not exhibit the most radiogenic composition. This probably reveals some early off-axis interactions between the mantle plume and the local DM. Such interaction, occurring during the relative rapprochement of a ridge and a hot spot, has been observed in some seamounts of the Foundation chain [*Maia et al.*, 2000]. It is therefore conceivable that the same process may have occurred when the early CDP seamounts formed. The second seamount generation (<2.1 Ma) displays much more variable isotopic signatures and the youngest seamount even exhibits the most extreme composition among our new data set. Apollinaire is therefore, in composition, the closest sample to ASP hot spot end-member. Considering those samples as representative of the bulk composition of the seamounts, we can explain this observation as follows: (1) the large old seamounts may result from larger degrees of melting, and therefore exhibit a more dilute enriched signature because of mixing with local depleted mantle melts and (2) the youngest seamounts, which formed above lithospheric cracks [*Janin et al.*, 2011], would result from lower degrees of melting of more enriched materiel left by the plume under or in the lithosphere. *Maia et al.* [2011] suggested an episodic activity of ASP mantle plume. In the frame of Maia et al. models, the youngest seamounts are related to the second pulse which constructed the ASP plateau [*Janin et al.*, 2011]. Some plume material could have been ponded underneath the plateau, enhancing melt eruption through a weaker lithosphere, and the construction of the young seamounts along the Capricorn and Australian plate diverging boundary. Such material migration can occur prior or after the plume melting, that is to say in a solid or liquid state. The survival of extreme isotope signature, and the survival small scales heterogeneities within a single seamount, rather suggest a solid state for

the migration of ASP plume material under the lithosphere. Indeed, melt transport would have contributed to a better homogenization within the material and then diluted such extreme signature. The plume melting then occurs in relationship with tectonic weaknesses of the lithosphere.

[33] As established earlier, the hot spot must have a Pb isotopes composition at least as radiogenic as Apollinaire, but can also be more radiogenic as well. We will try now to use the shift in $^{208}Pb/^{204}Pb$ for a given $^{206}Pb/^{204}Pb$ of the ASP plateau samples to bring further constraints on the composition of the plume end-member. In Figure 5, the dispersion of the ASP plateau (this study and *Nicolaysen et al.* [2007] for the present ridge samples) can be used to define another linear trend with a flatter slope passing through the most radiogenic samples of the plateau in $^{208}Pb/^{204}Pb$ for a given $^{206}Pb/^{204}Pb$: on axis and slightly off-axis samples, Amsterdam island [*Doucet et al.*, 2004], PLU DR24 which is a small seamount on 1.5 Ma old crust (red dotted line in Figure 5). In other words, the youngest ASP plateau samples require the addition of a third component (discussed in section 6.2). We can speculate that the influence of the plume composition is present in both trends, and therefore that its Pb composition is likely to be represented by the intercept of both trends (Figure 5): $^{206}Pb/^{204}Pb$ = 19.7 and $^{208}Pb/^{204}Pb$ = 40. This leads us to discuss now the composition of ASP plume and its origin. To facilitate the reading of the diagrams, we decided to give the samples a color code following the influence (or not) of the PLU DR24 components. The plateau samples, lying on the trend between ASP end-member and the Indian DM in the $^{208}Pb/^{204}Pb$ versus $^{206}Pb/^{204}Pb$, are in blue squares and called ASP-DM trend in all diagrams; while the samples enriched in $^{208}Pb/^{204}Pb$ are in red circles and called ASP-DR24 trend. The CDP samples remain apart with yellow diamonds.

6.1.2. ASP End-Member, Composition and Link With Pelagic Sediments

[34] In the other isotopic systems, the CDP samples exhibit a relative homogeneity, when compared to Pb isotopic ratios (Figure 4), which suggest less fractionation of Rb/Sr, Sm/Nd and Lu/Hf parent/daughter ratios. The plume component deduced from this study compares well with the C component from [*Hanan and Graham*, 1996] in terms of $^{206}Pb/^{204}Pb$, $^{87}Sr/^{86}Sr$, $^{143}Nd/^{144}Nd$, $^{176}Hf/^{177}Hf$. However, it requires a mantle source with a higher $^{208}Pb/^{204}Pb$, which suggests a higher time-integrated Th/U ratio. Two major components have been shown to have high $^{208}Pb/^{206}Pb$ at a low $^{206}Pb/^{204}Pb$: pelagic sediments and granulitic lower continental crust [*Ben Othman et al.*, 1989; *Rudnick and Goldstein*, 1990; *Rudnick and Fountain*, 1995; *Plank and Langmuir*, 1998].

[35] The circum-Indian Ocean granulites (African, Australian, Indian) have a high $^{87}Sr/^{86}Sr$ and low $^{143}Nd/^{144}Nd$ and $^{206}Pb/^{208}Pb$ ratios ($^{143}Nd/^{144}Nd$ < 0.5124 and $^{206}Pb/^{208}Pb$ < 18 [*Cohen et al.*, 1984; *Huang et al.*, 1995]) as seen in Figure 6. Consequently, none of them have the required composition to account for the ASP plume isotopes composition.

[36] Pelagic sediments have high Th/U evolving to high $^{208}Pb/^{204}Pb$ ratios but their low U/Pb ratio limits the increase of $^{206}Pb/^{204}Pb$ through time with a range of composition of $^{206}Pb/^{204}Pb$ < 19 [*Ben Othman et al.*, 1989; *Plank and Langmuir*, 1998; *Stracke et al.*, 2003]. Pelagic sediments' time-integrated $^{206}Pb/^{204}Pb$ is thus too low to account for ASP plume composition. At global scale, it is established that Pb is more mobile during subduction than U and *a fortiori* than Th [*Johnson and Plank*, 1999]. Therefore, the recycled crustal material (magmatic section + sediments) must have elevated U-Th/Pb ratios and evolve through time to a higher $^{206}Pb/^{204}Pb$. *Chauvel et al.* [1992] calculated that oceanic crust recycled through a 0.5 to 2 Ga process could reach a Pb ratio of $^{206}Pb/^{204}Pb$ = 19 to 23. Following the model of *Chauvel et al.* [1992], recycled pelagic sediments can therefore account for ASP plume composition into the Pb-Pb isotopes space as well as Sr-Nd isotopes space. Indeed, the CDP field in the Sr-Nd isotopic diagram (Figure 4) is quite homogeneous when compared with the ASP plateau samples. Consequently, they result from a process that do not create Rb/Sr and Sm/Nd decoupling, hence no enrichment in the parent-daughter ratios through isotopic decay. *Kelley et al.* [2005] have established that Rb is highly mobile during subduction, generating low Rb/Sr ratios in any recycled material. Consequently, old recycled pelagic material mixed with an average MORB mantle is a possible source for the composition of the CDP samples, according to their $^{87}Sr/^{86}Sr$ signature.

[37] Regarding Lu/Hf and Sm/Nd ratios, *Patchett et al.* [1984] and *Vervoort et al.* [1999] demonstrated that pelagic sediments display a significant decoupling between them and thus in Hf and Nd

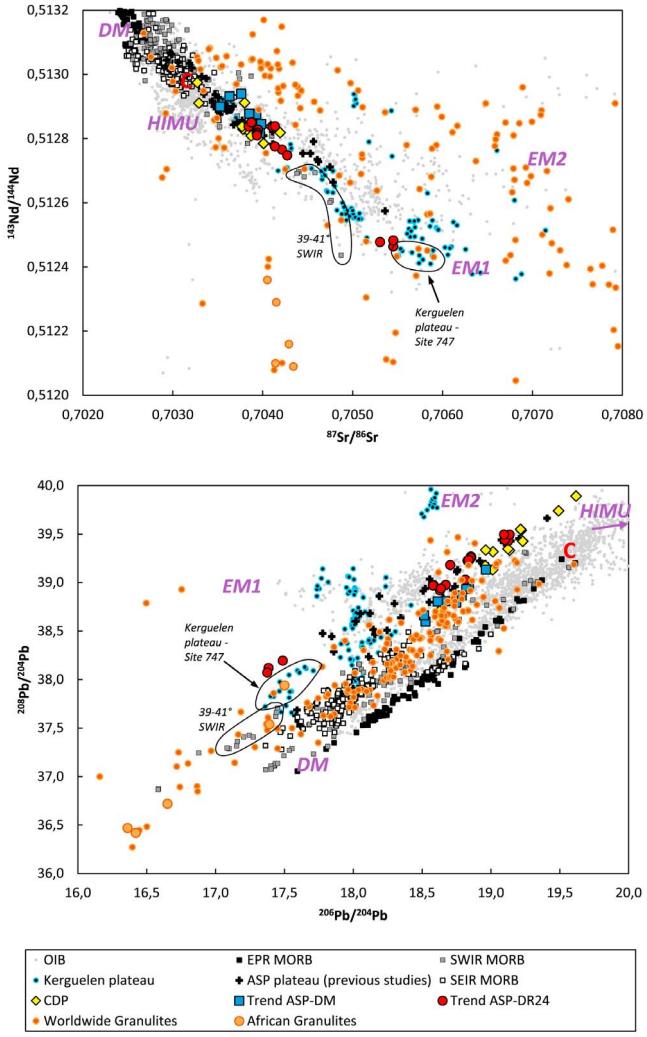

Figure 6. ASP plateau and CDP samples $^{87}Sr/^{86}Sr$ versus $^{143}Nd/^{144}Nd$ and $^{208}Pb/^{204}Pb$ versus $^{206}Pb/^{204}Pb$ diagrams compared to worldwide (compiled files from the GEOROC database available at http://georoc.mpch-mainz.gwdg.de/georoc/) and African granulites [*Cohen et al.*, 1984; *Huang et al.*, 1995].

isotopes. Pelagic sediments, which are deprived in Hf-rich zircons, have higher Lu/Hf ratios relatively to their Sm/Nd ratios [*Chauvel et al.*, 2008]. Through isotopic decay, these constraining parent-daughter ratios lead to isotopic compositions displaced above the mantle field in Hf-Nd space. Old recycled pelagic sediments would therefore have Nd and Hf isotopic compositions displaced to the left of the mantle array in Figure 4, where the CDP samples are clearly displaced above the mantle array. Mixing of old pelagic material with an average mantle can therefore account for the composition of the CDP samples in Nd-Hf isotopic space (Figure 4). This supports the presence of old pelagic sediments in ASP plume end-member, as suggested by the Pb isotopic ratios.

[38] To summarize, the incorporation of old recycled pelagic sediments into the mantle can account for ASP plume Hf-Pb-Sr-Nd isotope signatures. Nevertheless, those sediments were recycled within the mantle, together with the magmatic section of the slab, i.e. oceanic crust. In addition, this composite component must have been mixed later within the Indian Ocean upper mantle. The following paragraph will discuss the proportions of such mixing to reproduce the ASP sample compositions.

6.1.3. Mixing Model and Proportion of Pelagic Sediments

[39] Recycling of oceanic crust in the mantle during subduction processes is commonly

considered as having created the HIMU-like end-member [*Hofmann*, 2004] but this recycling may be accompanied by small amount of sediments. The HIMU end-member is characterized by a high time-integrated U/Th (and high U/Pb) resulting in a high $^{206}Pb/^{204}Pb$ for a given $^{208}Pb/^{204}Pb$ (Figures 4 and 5). The ASP end-member does not have such characteristics but derives from a time-integrated high Th/U. Nevertheless, *Chauvel et al.* [1992] demonstrated than only a few percents of sediments in the recycled crust-sediments mixture would mask the characteristic radiogenic Pb signature of the recycled crust (i.e., the HIMU end-member). Consequently, it is likely that oceanic crust recycled with a small amount of sediments will not develop a HIMU signature. A mixture of basalt + pelagic sediments evolves in the Pb-Pb space toward (1) a $^{206}Pb/^{204}Pb$ ratio that is lower than the one which would be achieved by the oceanic crust alone and (2) to higher $^{208}Pb/^{204}Pb$ than those of present-day MORB, which are the characteristics of ASP plume end-member (Figure 5). Recycled oceanic crust mixed with a small amount of pelagic sediments could account for ASP plume composition. Using the method of *Chauvel et al.* [1992], we determined that less than 1% of pelagic sediments with oceanic crust recycled through a 1,5 Ga old subduction process could account for the CDP samples compositions. Such timing of recycling confirms the deep-seated ASP plume evidenced by *Janin et al.* [2010, 2011] using geochronological data.

[40] The interaction between ASP end-member (with a "pelagic sediment + oceanic crust" signature) and the Indian upper mantle can be constrained using the mixing equation of *Langmuir et al.* [1978]. The resulting mixing lines (Figure 7) show that the incorporation of 10% (Apollinaire seamount) to 50% of Indian upper mantle within the mantle plume could account for the CDP samples dispersion. Some of the ASP-DM trend lies over this single mixing line between ASP plume and the Indian upper mantle. Their composition requires the incorporation of 25% to 55% of Indian DM within ASP plume.

[41] However, at the scale of the plateau, the lavas exhibit a second trend shifted toward higher $^{208}Pb/^{204}Pb$ for a given $^{206}Pb/^{204}Pb$. This trend implies the addition of a third end-member (in addition to ASP plume and the Indian upper mantle) to account for ASP plateau samples distribution. The nature of this end-member is discussed in the following paragraph.

6.2. PLU-DR 24 and Samples With a DUPAL-Flavor

6.2.1. Plume-Ridge Interaction and Influence of the DUPAL Component on the ASP Plateau Basalts

[42] In Figure 4, some plateau samples are displaced toward higher $^{208}Pb/^{204}Pb$ for a given $^{206}Pb/^{204}Pb$ and belong to the ASP-DR24 trend in Figure 5. Those samples, together with J1 and J2 SEIR segment (the segments crossing the ASP plateau, i.e. small black crosses in Figure 4) samples (data from *Nicolaysen et al.* [2007]), require the addition of a rather "homogeneous" third component to the mixing between ASP plume and the Indian upper mantle. The extreme samples of this trend is PLU DR-24 with a $^{208}Pb^*/^{206}Pb^* = 1.07$ ($^{208}Pb^*/^{206}Pb^* = (^{208}Pb/^{204}Pb - 29.475)/(^{206}Pb/^{204}Pb - 9.307)$ i.e., the measured $^{208}Pb/^{206}Pb$ ratios corrected from primordial Pb. A $^{208}Pb^*/^{206}Pb^* > 1$ correspond to an enrichment in ^{208}Pb for a given ^{206}Pb). PLU DR 24 and the samples delineating the ASP-DR24 trend exhibit higher $^{87}Sr/^{86}Sr$ and $^{208}Pb/^{206}Pb$ and lower $^{143}Nd/^{144}Nd$ at a given $^{206}Pb/^{204}Pb$, including some ASP plateau lavas from previous studies [*Dosso et al.*, 1988; *Doucet et al.*, 2004; *Nicolaysen et al.*, 2007]. This third component could be either related to the ASP plume itself (intrinsic heterogeneity) or to some heterogeneity of the Indian upper mantle. As presented in previous sections, ASP-DR24 trend samples are found in the thicker part of the ASP plateau (i.e., related to the interaction with the ridge) while the CDP samples are related to the ASP intraplate activity (>8 Ma) and do not exhibit, for most of them, a DR24-flavor. *Graham et al.* [1999] and *Nicolaysen et al.* [2007] revealed that the H segment of the SEIR was contaminated by ASP hot spot derived material. However, they do not exhibit any PLU DR24 flavor either, which suggests that the PLU DR24 end-member is not related to ASP plume material. *Ito et al.* [2003] demonstrated that, in a ridge-hot spot interaction system, the plume signature dominates the composition of the resulting lavas. PLU DR6 and PLU DR34 represent the current and old on-axis magmatic phases respectively, and none of them appear as the extreme DR24-like component recorded on ASP plateau, which confirms that the PLU DR24

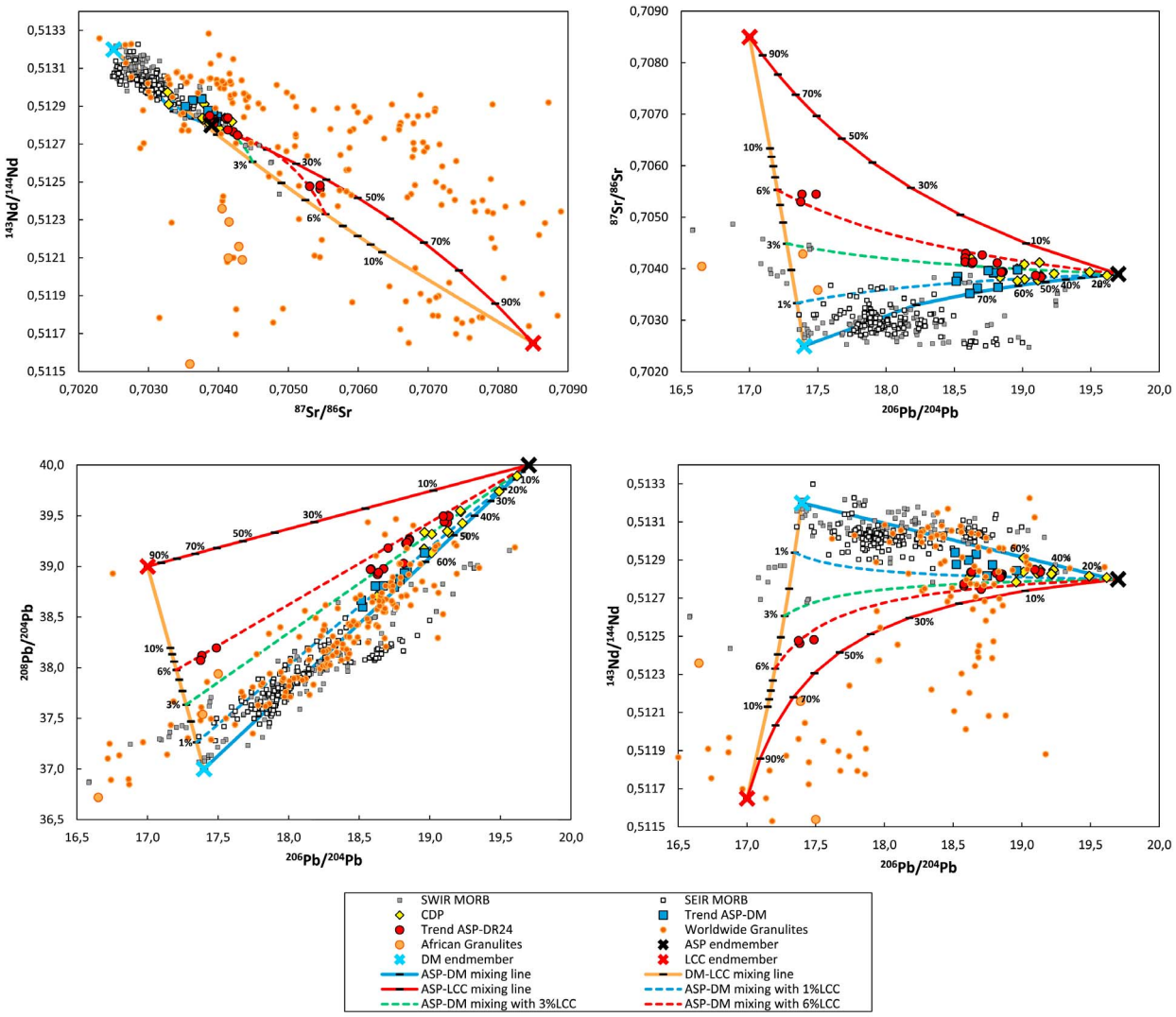

Figure 7. Mixing model between the Indian DM (blue cross), ASP hot spot end-member (black cross) and a lower continental crust component (red cross). The ASP plateau and CDP samples are grouped in CDP (small yellow diamonds), ASP-DM trend (blue squares) and ASP-DR24 trend (red circle) – see text for discussion. Orange and brown circles represent African and worldwide granulites, respectively. PLU DR24 composition tends to African granulites, which provides a third end-member to explain ASP plateau geochemical variations. The chosen compositions are detailed below. Marks on the mixing lines are graduated from 10 to 100% except for DM-LCC mixing (graduations from 1 to 10%). The LCC end-member composition is $^{87}Sr/^{86}Sr = 0.7085$, [Sr] = 500 ppm, $^{143}Nd/^{144}Nd = 0.51165$, [Nd] = 20 ppm, $^{206}Pb/^{204}Pb = 17$, $^{208}Pb/^{204}Pb = 39$, [Pb] = 15 ppm, values adapted from the literature (included African granulites by *Cohen et al.* [1984] and *Huang et al.* [1995]) The ASP hotpot composition is $^{87}Sr/^{86}Sr = 0.7039$, [Sr] = 600 ppm, $^{143}Nd/^{144}Nd = 0.5128$, [Nd] = 40 ppm, $^{206}Pb/^{204}Pb = 19.7$, $^{208}Pb/^{204}Pb = 40$, [Pb] = 5 ppm, values adapted from the CDP samples. The Indian DM composition is $^{87}Sr/^{86}Sr = 0.7025$, [Sr] = 50 ppm, $^{143}Nd/^{144}Nd = 0.5132$, [Nd] = 1 ppm, $^{206}Pb/^{204}Pb = 17.4$, $^{208}Pb/^{204}Pb = 37$, [Pb] = 1 ppm, values adapted from the literature [*Hofmann*, 2004, and references therein].

signature is related to heterogeneity within the Indian mantle. In addition, those characteristics are similar to those of 39–41°E segments of the SWIR, as well as DUPAL-like localities. Consequently, the origin of PLU DR24 characteristics seems related to a global process. Therefore, the nature of PLU DR24 component must be discussed within the frame of the DUPAL anomaly origin. The DUPAL component has been attributed to diverse origins including, among others, ancient recycled sediments

[*Rekhämper and Hofmann*, 1997] and delaminated continental crust [*Douglass et al.*, 1999; *Escrig et al.*, 2004; *Hanan et al.*, 2004; *Meyzen et al.*, 2005]. In the following paragraph, we will discuss the various assumptions evoked for the nature of PLU DR24 component and the origin of ASP-DR 24 trend characteristics.

6.2.2. The Lower Continental Crust as an Origin for the DUPAL Anomaly

[43] The literature data did not reach a consensus about the origin of the DUPAL anomaly [*Dupré and Allègre*, 1983; *Hamelin and Allègre*, 1985, 1986; *Mahoney et al.*, 1992; *Chauvel and Blichert-Toft*, 2001; *Frey et al.*, 2002; *Hanan et al.*, 2004; *Ingle et al.*, 2003; *Janney et al.*, 2005; *Meyzen et al.*, 2005; *Regelous et al.*, 2009]. Therefore, we used trace elements contents to better constrain the mantle source of PLU DR24. As shown in Figure 4, PLU DR24 lavas have high Sr and Eu relatively to REE of similar incompatibility with Sr/Nd and Eu/Eu* ratios higher than in other plateau samples. Sr and Eu are highly compatible in plagioclase and Ba and Sm are less incompatible in plagioclase than Nb and Hf respectively, therefore, plagioclase-rich components have relatively high Ba/Nb and Sm/Hf, like PLU DR24. The plagioclase-rich source is also illustrated by the Ba/La versus La diagram (Figure 8) where PLU DR24 samples exhibit an enrichment in Ba. These characteristics might thus result either (1) from the assimilation of plagioclase or plagioclase-rich cumulates within the oceanic lithosphere by N-MORB or (2) from the presence of a plagioclases-rich component in the mantle source. The following paragraph will discuss the different models for those characteristics as proposed in the literature for the DUPAL anomaly origin.

6.2.2.1. Oceanic Crust?

[44] Along the pathway from the mantle source to the surface, the magmas cross the oceanic lithosphere including the oceanic crust. Gabbros, rich in plagioclase cumulates, represent the lower part of the oceanic crust and the assimilation of gabbro has been evoked to explain the plagioclase signature of lavas from Iceland [*Hemond et al.*, 1993] or from the Kerguelen plateau [*Yang et al.*, 1998]. The isotopic signature of the oceanic crust is related to its mantle source and is mainly accessible through the MORB isotopic composition. The $^{87}Sr/^{86}Sr$ ratio of PLU DR24 is higher than those of Indian MORB, and therefore, is not readily explained by the eventual assimilation of oceanic gabbros although gabbros could be contaminated easily by seawater Sr $^{87}Sr/^{86}Sr$ (=0.7092) and then acquire higher $^{87}Sr/^{86}Sr$ to account for PLU DR24 signature. However, seawater contamination will move the data point to the right of the mantle array at constant $^{143}Nd/^{144}Nd$. On the contrary, PLU DR24 lavas have relatively low $^{143}Nd/^{144}Nd$ and lie close to the mantle array, excluding the assimilation of altered oceanic gabbros as a potential source. Similarly, the assimilation of gabbro would not explain the higher $^{208}Pb/^{204}Pb$ for a given $^{206}Pb/^{204}Pb$ of PLU DR24 since the Indian Oceanic crust does not exhibit such extreme compositions. The plagioclase signature of ASP-DR24 trend samples must therefore be inherited from the mantle source.

[45] High Sr/Nd ratios in lavas of some intraplate islands have been interpreted as an evidence for recycled oceanic gabbro under the form of eclogite within the mantle [*Hofmann and Jochum*, 1996; *Chauvel and Hémond*, 2000; *Sobolev et al.*, 2000]. Oceanic gabbros have low Rb/Sr, U/Pb, Th/Pb and Th/U ratios [*Hart et al.*, 1999], which over time will result in relatively unradiogenic Sr and Pb istopes ratios (ex: $^{208}Pb/^{204}Pb < 37$ [*Stracke et al.*, 2003]) unlike PLU DR24 ($^{208}Pb/^{204}Pb > 38$). Consequently, oceanic crust can be excluded as a possible source of the PLU DR24 lavas neither through assimilation by the ascending melts nor as recycled crust within the mantle.

6.2.2.2. Pelagic Sediments?

[46] The PLU DR24 isotopic composition is intermediate between the Indian MORB and the EM1-end-member. The trace elements and isotopic characteristics of some EM1-type lavas have been attributed to the melting of a mantle source containing a small amount of ancient subducted pelagic sediments [*Hamelin and Allègre*, 1985; *LeRoex et al.*, 1989; *Weaver*, 1986, 1991; *Andres et al.*, 2002]. The composition of PLU DR24 samples is comparable to lavas of the 39–41°E SWIR segment, but with a higher $^{208}Pb/^{206}Pb$. *Meyzen et al.* [2005] showed that none of the sediments has the U/Pb and Th/Pb ratios leading through time to the compositions of the peculiar basalts from the 39–41°E SWIR segment, especially to its enrichment in $^{208}Pb/^{204}Pb$. On the same basis, we exclude pelagic sediments as the source of PLU DR24 lavas. The low Sm/Nd and high Lu/Hf of pelagic sediments will create through time a decoupling in the isotopic compositions, which will be displaced above the mantle array in Hf-Nd space [*Patchett et al.*, 1984; *Vervoort et al.*, 1999]. However, PLU

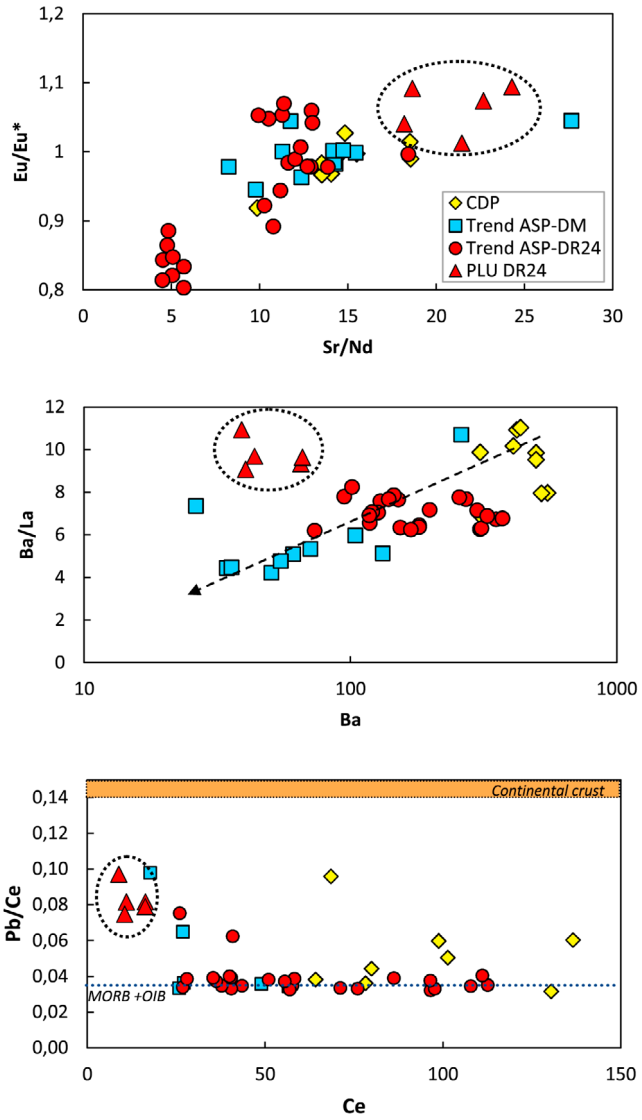

Figure 8. Variations of Sr/Nd with Eu/Eu*, of Ba/La with Ba (in ppm) and variation of Pb/Ce with Ce (in ppm). Eu/Eu* is defined as $Eu_N/(Sm_N*Gd_N)^{0,5}$ where N indicated abundances normalized to Chondrites [*McDonough and Sun*, 1995]. PLU DR24 samples exhibit a higher Sr/Nd and Eu/Eu*, as well as a higher Ba/La suggesting the presence of plagioclases in the lavas source. Its high Pb/Ce indicates a continental origin for the PLU DR24 geochemical signature. 2σ error bars are smaller than symbol size.

DR24 samples are located on the mantle array in such diagram (Figure 6), therefore excluding pelagic sediments as the source of PLU DR24 lavas. In addition, pelagic sediments would not account for the PLU DR24 trace elements compositions since, for example, the average Sr/Nd ratio of sediments recycled through subduction process is 12, which is too low to account for the Sr/Nd ratio of PLU DR24 (>18). Consequently, the incorporation on pelagic sediments in the mantle source, which not account for PLU DR24 signature, can be excluded as the origin of ASP-DR24 trend.

6.2.2.3. Metasomatic Subarc Mantle

[47] In the Indian Ocean, an isotopic signature resembling PLU DR24 characteristics is also found in the Australian-Antarctic Discordance (AAD) basalts. *Kempton et al.* [2002] argued that the distinct signature of the AAD basalts may be caused

by the presence of recycled material arising from subduction modified mantle embedded within the shallow asthenosphere. Consequently, an alternative origin for PLU DR24 source is the incorporation of subduction modified subarc mantle. Such mantle would then have undergone metasomatism and melting during subduction leading to peculiar characteristics before being recycled into the mantle. *Kempton et al.*'s [2002] model is based on Hf-Nd systematics and could account for the composition of PLU DR24 in Hf and Pb isotopes. In addition, the high mobility of Pb within fluids during subduction processes would lead to high Pb/Ce in the metasomatized mantle, in agreement with the high Pb/Ce observed in PLU DR24 samples. However, the incorporation of metasomatized mantle is inconsistent with the Pb isotopes. *Meyzen et al.* [2005] calculated the evolution through time of such material and established that they were not a plausible end-member to account for the $^{208}Pb/^{204}Pb$ enrichment seen in the peculiar basalts from the 39–41°E SWIR segment, whatever the age of the subduction was. Since PLU DR24 lavas have even higher $^{208}Pb/^{204}Pb$ for the same $^{206}Pb/^{204}Pb$ than 39–41°E SWIR basalts, metasomatic processes are unlikely to explain the PLU DR24 end-member as well. Metasomatic sub-arc mantle may also be excluded as a possible source component for ASP-DR24 trend signature.

6.2.2.4. Lower Continental Crust

[48] As discussed above, the trace elements compositions of PLU DR24 lavas show that a plagioclase-rich component may have contributed to the source of the lavas. Plagioclase is known to be an important phase from the lower continental crust (LCC) and such rocks exhibit high Sr/Nd and Eu/Eu* [*Rudnick et al.*, 1986; *Rudnick and Fountain*, 1995; *Rudnick and Gao*, 2003]. Throughout the 1980s, Hofmann, Jochum, and coworkers studied a series of trace element ratios that are globally more or less uniform in both MORBs and OIBs [*Hofmann and Jochum*, 1996; *Hofmann*, 2004, and references therein]. Pb/Ce is one of those with a range of about 0.033 but which is much higher by factors of about 5–10 in the continental crust [*Hofmann et al.*, 1986; *Hofmann*, 2004]. PLU DR24 exhibits a Pb/Ce anomaly suggesting a continental origin (Figure 8). Whether or not the LCC is a suitable component for PLU DR24 lavas can be assessed from the isotopic composition of lower crustal granulite xenoliths (Figure 6). The isotopic compositions of such xenoliths vary from one region to another but at a worldwide scale most of the granulites are characterized by higher $^{208}Pb/^{204}Pb$, higher $^{87}Sr/^{86}Sr$ and lower $^{143}Nd/^{144}Nd$ for a given $^{206}Pb/^{204}Pb$ when compared to Indian MORBs. In addition, a few granulite sites, such as Southern Africa or Tanzania, are characterized by extremely low $^{206}Pb/^{204}Pb$ [*Cohen et al.*, 1984; *Huang et al.*, 1995]. These African granulitic xenoliths have a composition close to the hypothetical end-member required in ASP-DR24 trend in Pb-Pb isotopes space and the dispersion observed in Sr-Nd or Sr-Pb spaces may easily be explained by intrinsic variability in the granulites compositions at a worldwide scale. This assumption is also coherent with literature data, which pointed garnet fractionation (a possible major phase of granulites) as an explanation for the high εHf of the Indian MORBs [*Hanan et al.*, 2004; *Graham et al.*, 2006].

[49] Delamination of LCC represents an alternative mechanism for recycling continental material into the convective upper mantle [*Arndt and Goldstein*, 1989; *Turcotte*, 1989; *Kay and Kay*, 1993; *Regelous et al.*, 2009]. Remnants of LCC from the craton margin could have been stripped off and incorporated into the Indian upper mantle during the breakup of Gondwana around 120 Myr ago [*Escrig et al.*, 2004]. Similar scenarios have been proposed by several investigators to explain the compositions of lavas with DUPAL characteristics, such as PLU DR24, formed on spreading centers [*Mahoney et al.*, 2002; *Hanan et al.*, 2004; *Escrig et al.*, 2005; *Janney et al.*, 2005; *Meyzen et al.*, 2005] and intraplate oceanic volcanoes [*Douglass et al.*, 1999; *Mahoney et al.*, 1996; *Borisova et al.*, 2001; *Frey et al.*, 2002; *Regelous et al.*, 2009]. In addition, PLU DR24 compositions are really closed to data from site 747 from the Kerguelen plateau [*Frey et al.*, 2002] and from Heard Island [*Barling et al.*, 1994] (Figures 4 and 5). The authors of those studies reached a similar interpretation about the origin of such signature. In particular, *Frey et al.* [2002], using similar trace element ratios, suggested that lavas from site 747 (Kerguelen plateau) have compositions originating from a plagioclase-rich component, similarly to this study. In site 747, the trace elements composition of the lavas display much higher Sr, Eu and Ba, clearly indicating a strong crustal input. In this study, this trace element signature seems to be a little bit more diluted in the PLUDR24 samples but remains significant. In petrography as well as in isotopic composition the LCC remains the most likely component responsible for PLU DR24 origin.

[50] The required contribution of the lower continental crust, in ASP lavas, and its implications, will be evaluated in the following paragraph.

6.2.3. Proportion of LCC

[51] ASP plateau sample dispersion is thus related to a three components mixing: (1) ASP plume, (2) the Indian DM upper mantle, and (3) some lower continental crust layers probably delaminated during the Gondwana break-up. The proportions of the first two components have been evaluated in section 6.1.1. To modeled the mixing between the three components the following three end-members are required: (1) high $^{143}Nd/^{144}Nd$, low $^{87}Sr/^{86}Sr$ -$^{206}Pb/^{204}Pb$-$^{208}Pb/^{204}Pb$ Indian DMM, (2) an ASP end-member close to the C component from *Hanan and Graham* [1996] but with a higher $^{208}Pb/^{204}Pb$, and (3) a low $^{206}Pb/^{204}Pb$-$^{143}Nd/^{144}Nd$ component with relatively high $^{87}Sr/^{86}Sr$ and $^{208}Pb/^{204}Pb$. As discussed above, we argue that the origin of the DUPAL flavor (low $^{206}Pb/^{204}Pb$ – high $^{208}Pb/^{204}Pb$) is derived from the lower continental crust, which was delaminated and incorporated into the upper mantle.

[52] The end-member required for PLU DR24 extreme composition resembles to African Granulites, which are nevertheless not even high enough in $^{208}Pb/^{204}Pb$ or $^{87}Sr/^{86}Sr$ (see Figure 6). At a worldwide scale, the LCC component is highly heterogeneous, and extremely high $^{208}Pb/^{204}Pb$ ratios for a given $^{206}Pb/^{204}Pb$ have been found in Australia or north America [*Leeman et al.*, 1985; *Tilton and Bareiro*, 1980; *Rudnick and Goldstein*, 1990; *Putirka et al.*, 2009]. Since granulitic xenoliths are surely not representative for the whole LCC, we have chosen an ad hoc LCC end-member composition close to the African granulites composition [*Cohen et al.*, 1984; *Huang et al.*, 1995] but slightly higher in $^{208}Pb/^{204}Pb$ (=39, seen in Figure 7 caption). This allowed us to establish an order of magnitude for the LCC end-member contribution into the mixing, using the equation of *Langmuir et al.* [1978], to account for the ASP samples distribution (mixing lines in Figure 7). Approximately 0–3% of LCC explain the ASP plateau distribution when added to a simple Indian DM-ASP plume mixing (discussed in section 6.1), with a maximum contribution of 6% to account for the composition of the extreme sample PLU DR24 (Figure 7). The calculated proportions are comparable for all the isotopes (see Figure 7 caption for the concentration and compositions used in the mixing models).

[53] Mixing models for the whole Indian Ocean usually invoke a two stage mixing event, in which the asthenosphere experienced a widespread contamination by a low $^{206}Pb/^{204}Pb$, before being mixed with OIB type material [*Hanan and Graham*, 1996; *Douglass and Schilling*, 2000; *Chauvel and Blichert-Toft*, 2001; *Escrig et al.*, 2004; *Meyzen et al.*, 2005; *Rooney et al.*, 2012]. Our model also consists in a two-stage and three components involving the lower continental crust as low $^{206}Pb/^{204}Pb$ component. In our calculation, a maximum of 1% of recycled lower crust in the Indian DM is sufficient to explain the Indian Ocean MORB distribution. This is in agreement with previous studies which have attributed the DUPAL anomaly to lower continental crust in the Indian [*Arndt and Goldstein*, 1989; *Frey et al.*, 2002; *Escrig et al.*, 2004; *Hanan et al.*, 2004; *Meyzen et al.*, 2005] and South Atlantic Oceans [*Kamenetsky et al.*, 2001; *Escrig et al.*, 2005; *Regelous et al.*, 2009].

[54] However, although the proposed model can account for most of the isotopic features of ASP plateau lavas, the $^{143}Nd/^{144}Nd$ versus $^{87}Sr/^{86}Sr$ trend requires a larger amount of high $^{87}Sr/^{86}Sr$ material. These features might be explained if the low $^{206}Pb/^{204}Pb$ – high $^{208}Pb/^{204}Pb$ (i.e. the LCC component) and/or if the ASP end-member is more heterogeneous than considered in the mixing model. Even if such small scale variations cannot be perfectly modeled, this conclusion would therefore be consistent with the isotopic characteristics of granulites as well as others mantle plumes at a worldwide scale. Granulites, as well as mantle plumes, are indeed known to be more or less heterogeneous reservoirs. Consequently, some small dispersion in the mixing models remains plausible and allows us to give an order of magnitude of each end-member required in ASP plateau samples (1) 45% to 75% of ASP plume derived material and (2) 25% to 55% of Indian DM within 0–6% of LCC layers included within.

[55] Previous studies revealed the homogeneity of Amsterdam and St. Paul lavas isotopic compositions, respectively. A new data set on Amsterdam lavas is consistent with those results [*Janin et al.*, 2010]. This homogeneity seems paradoxical when compared to the complete ASP plateau data set, and small scale heterogeneities observed on some seamounts. A few samples of Amsterdam Island have been dated. *Carvallo et al.* [2003] provided ages of 18 +/– 9 ka and 26 +/15 ka and *Janin* [2010] of 19 +/– 7 Ka. Others samples revealed themselves too young to be dated by K-Ar [*Janin*, 2010], implying that they were younger than 50 ka. According to their geographical location, those samples belong to the recent activity of Amsterdam Island, i.e. La Dives volcano. The apparent homogeneity in Amsterdam Island lavas may result from the presence of intermediate

magmatic chambers into the plateau structure and is thus more probably due to a bias of sampling than to an homogeneous lava source through time.

7. Conclusion

[56] The ASP plateau results from the interaction between the ASP plume and the SEIR, and its lava compositions present a strong variability in Sr, Nd, Pb and Hf isotopic ratios, requiring the incorporation of three main components: (1) the ASP plume, (2) the Indian DM and (3) a clear DUPAL input. The volcanic Chain of the Dead Poets (CDP), lies to the northward tip of the plateau and is related to the plume intraplate activity. The study of the ASP plateau and the CDP reveals that the ASP plume is composed of oceanic crust and pelagic sediments recycled within the mantle through a 1.5 Ga subduction event. Such ancient recycling age suggests that the ASP plume is a deep plume and supports the conclusion of *Janin et al.* [2011] based on geochronological data.

[57] The ASP plateau lavas have a composition reflecting the interaction between ASP plume, and the Indian MORB mantle, with some strong DUPAL input. The study of PLU DR24, the extreme DUPAL-like sample, and of the entire plateau data set reveals the existence of a continental component into the lava source. This continental component exhibits isotopic compositions resembling to those of other locations in the Indian Ocean and of African granulites. We thus interpret the shift of ASP samples toward PLU DR24 as the influence of a lower continental crust component, probably delaminated during the Gondwana breakup and incorporated into the Indian upper mantle around 120 Ma ago. Only 0–3% of recycled LCC is sufficient to explain the ASP plateau lavas by derivation from a simple Indian DM-ASP plume mixing, while a maximum of 6% is required to account for the composition of the extreme sample.

[58] At a global scale, the lower continental crust is a possible reservoir for the DUPAL anomaly origin and our data support this model. Only 0–1% recycled lower crust within the Indian DM can account for the Indian Ocean MORB distribution, when mixed with a Pacific-like upper mantle.

[59] The three end-members involved in ASP plateau lavas (plume, upper mantle and lower continental crust) and their mixing in various proportions (45% to 75% of ASP plume + 25% to 55% of Indian DM within 0% to 6% of LCC layers included within) results in a large geochemical variability in the plateau samples. Consequently, the apparent composition homogeneity of Amsterdam Island, an aerial summit of the plateau, is surprising and may result from the presence of intermediate magmatic chambers into the plateau structure.

Acknowledgments

[60] The PLURIEL cruise was funded by the "Ministère de l' Enseignement Supérieur et de la Recherche" through CNRS - INSU and IPEV and by the program EXTRAPLAC. CNRS - INSU through the program SEDIT funded most of the work on the data presented here. We thank Captain F. Duchesne and the crew of RV Marion Dufresne II and the engineers of IPEV for their help with the acquisition of the data during the cruise, and Arnaud Agranier and Clément Lacorte for their help during the lab work. We are also indebted to Olivier Gilbert, a TAAF volunteer, who performed Amsterdam Island sampling. MJ would like to thank Catherine Chauvel for her advices and for provided valuable insights, and Thomas Boulesteix for the improvements he has brought to the final paper. We would like to thank the editor Louis Derry for his careful editing and we are also indebted to two anonymous reviewers; their comments largely improved the quality of this manuscript.

References

Abouchami, W., S. J. G. Galer, and A. W. Hofmann (2000), High precision lead isotope systematics of lavas from the Hawaiian Scientific Drilling Project, *Chem. Geol.*, *169*, 187–209, doi:10.1016/S0009-2541(00)00328-4.

Andres, M., J. Blichert-Toft, and J. G. Schilling (2002), Hafnium isotopes in basalts from the southern Mid-Atlantic Ridge from 40°S to 55°S: Discovery and Shona plume-ridge interactions and the role of recycled sediments, *Geochem. Geophys. Geosyst.*, *3*(10), 8502, doi:10.1029/2002GC000324.

Arndt, N. T., and S. L. Goldstein (1989), An open boundary between lower continental crust and mantle: Its role in crust formation and crustal recycling, *Tectonophysics*, *161*, 201–212, doi:10.1016/0040-1951(89)90154-6.

Barling, J., S. L. Goldstein, and I. A. Nicholls (1994), Geochemistry of Heard Island (southern Indian Ocean): Characterization of an enriched mantle component and implications for enrichment of the sub-Indian Ocean mantle, *J. Petrol.*, *35*, 1017–1053.

Barrat, J. A., A. Yamaguchi, R. C. Greenwood, M. Bohn, J. Cotten, M. Benoit, and I. A. Franchi (2007), The Stannern trend eucrites: Contamination of main group eucritic magmas by crustal partial melts, *Geochim. Cosmochim. Acta*, *71*(16), 4108–4124, doi:10.1016/j.gca.2007.06.001.

Ben Othman, D., W. M. White, and J. P. Patchett (1989), The geochemistry of marine sediments, island arc magma genesis and crust-mantle recycling, *Earth Planet. Sci. Lett.*, *94*, 1–21, doi:10.1016/0012-821X(89)90079-4.

Birck, J.-L. (1986), Precision K-Rb-Sr isotopic analysis: Application to Rb-Sr chronology, *Chem. Geol.*, *56*, 73–83, doi:10.1016/0009-2541(86)90111-7.

Blichert-Toft, J., C. Chauvel, and F. Albarède (1997), Separation of Hf and Lu for high-precision isotope analysis of rock samples by magnetic sector-muti-collector ICP-MS,

Contrib. Mineral. Petrol., *127*, 248–260, doi:10.1007/s004100050278.

Borisova, A. Y., B. V. Belyatsky, M. V. Portnyagin, and N. M. Sushchevskaya (2001), Petrogenesis of olivine-phyric basalts from the Aphanasey Nikitin Rise: Evidence for contamination by cratonic lower continental crust, *J. Petrol.*, *42*(2), 277–319, doi:10.1093/petrology/42.2.277.

Burnard, P. G., D. W. Graham, and K. A. Farley (2002), Mechanisms of magmatic gas loss along the Southeast Indian Ridge and the Amsterdam–St. Paul Plateau, *Earth Planet. Sci. Lett.*, *203*, 131–148, doi:10.1016/S0012-821X(02)00828-2.

Cannat, M., et al. (1999), Mid-Atlantic Ridge–Azores hotspot interactions: Along-axis migration of a hotspot-derived event of enhanced magmatism 10 to 4 Ma ago, *Earth Planet. Sci. Lett.*, *173*, 257–269, doi:10.1016/S0012-821X(99)00234-4.

Carvallo, C., P. Camps, G. Ruffet, B. Henry, and T. Poidras (2003), Mono Lake or Laschamp geomagnetic event recorded from lava flows in Amsterdam Island (southeastern Indian Ocean), *Geophys. J. Int.*, *154*, 767–782, doi:10.1046/j.1365-246X.2003.01993.x.

Chauvel, C., and J. Blichert-Toft (2001), A hafnium isotope and trace element perspective on melting of the depleted mantle, *Earth Planet. Sci. Lett.*, *190*, 137–151, doi:10.1016/S0012-821X(01)00379-X.

Chauvel, C., and C. Hémond (2000), Melting of complete section of oceanic crust: Trace element and Pb isotopic evidence from Iceland, *Geochem. Geophys. Geosyst.*, *1*(2), 1001, doi:10.1029/1999GC000002.

Chauvel, C., A. W. Hofmann, and P. Vidal (1992), HIMU-EM: The French Polynesian connection, *Earth Planet. Sci. Lett.*, *110*, 99–119, doi:10.1016/0012-821X(92)90042-T.

Chauvel, C., E. Lewin, M. Carpentier, N. T. Arndt, and J.-C. Marini (2008), Role of recycled oceanic basalt and sediment in generating the Hf-Nd mantle array, *Nat. Geosci.*, *1*, 64–67, doi:10.1038/ngeo.2007.51.

Coffin, M. F., M. S. Pringle, R. A. Duncan, T. P. Gladczenko, M. Storey, R. D. Müller, and L. A. Gahagan (2002), Kerguelen hotspot magma output since 130 Ma, *J. Petrol.*, *43*(7), 1121–1137, doi:10.1093/petrology/43.7.1121.

Cohen, R. S., R. K. O'Nions, and J. B. Dawson (1984), Isotope geochemistry of xenoliths from East Africa: Implications for development of mantle reservoirs and their interaction, *Earth Planet. Sci. Lett.*, *68*, 209–220, doi:10.1016/0012-821X(84)90153-5.

Cotten, J., A. Le Dez, M. Bau, R. Maury, P. Dulsky, S. Fourcade, M. Bohn, and R. Brousse (1995), Origin and anomalous rare-earth element and yttrium enrichments in subaerially exposed basalts: Evidence from French Polynesia, *Chem. Geol.*, *119*, 115–138, doi:10.1016/0009-2541(94)00102-E.

Courreges, E. (2010), Plateau de St. Paul and Amsterdam et Nord Kerguelen: Interaction entre la dorsal Sud-est Indienne et deux point chauds, PhD dissertation, Univ. of Brest, Brest, France.

Dosso, L., H. Bougault, P. Beuzard, J. Y. Calvez, and J. L. Loron (1988), The geochemical structure of the Southeast Indian Ridge, *Earth Planet. Sci. Lett.*, *88*, 47–59.

Doucet, S., D. Weis, J. S. Scoates, V. Debaille, and A. Giret (2004), Geochemical and Hf-Pb-Sr-Nd Isotopic constraints on the origin of the Amsterdam–St. Paul (Indian Ocean) hotspot basalts, *Earth Planet. Sci. Lett.*, *218*, 179–195, doi:10.1016/S0012-821X(03)00636-8.

Douglass, J., and J.-G. Schilling (2000), Systematics of three-component, pseudo-binary mixing lines in 2D isotope ratio space representation and implications for mantle plume–ridge interaction, *Chem. Geol.*, *163*, 1–23.

Douglass, J., J.-G. Schilling, and D. Fontignie (1999), Plume-ridge interactions of the Discovery and Shona mantle plumes with the southern Mid-Atlantic Ridge (40°–55°S), *J. Geophys. Res.*, *104*(B2), 2941–2962.

Duncan, R. A., and M. Storey (1992), The life cycle of Indian Ocean hotspots, in *Synthesis of Results From Scientific Drilling in the Indian Ocean*, *Geophys. Monogr. Ser.*, vol. 70, edited by R. A. Duncan et al., pp. 91–103, AGU, Washington, D. C., doi:10.1029/GM070p0091.

Dupré, B., and C. J. Allègre (1983), Pb-Sr isotope variation in Indian Ocean basalts and mixing phenomena, *Nature*, *303*, 142–146, doi:10.1038/303142a0.

Escrig, S., F. Capmas, B. Dupré, and C. J. Allègre (2004), Osmium isotopic constraints on the nature of the DUPAL anomaly from Indian mid-ocean ridge basalts, *Nature*, *431*, 59–63, doi:10.1038/nature02904.

Escrig, S., P. Schiano, J.-G. Schilling, and C. Allègre (2005), Rhenium-osmium isotope systematic in MORB from the southern mid-Atlantic ridge (40–50°S), *Earth Planet. Sci. Lett.*, *235*, 528–548, doi:10.1016/j.epsl.2005.04.035.

Frey, F. A., et al. (2000), Origin ad evolution of a submarine large igneous province: The Kerguelen Plateau and Broken Ridge, southern Indian Ocean, *Earth Planet. Sci. Lett.*, *176*, 73–89, doi:10.1016/S0012-821X(99)00315-5.

Frey, F. A., D. Weis, A. Y. Borisova, and G. Xu (2002), Involvement of continental crust in the formation of the Cretaceous Kerguelen plateau: New perspectives from ODP Leg 120 sites, *J. Petrol.*, *43*(7), 1207–1239.

Gente, P., J. Dyment, M. Maia, and J. Goslin (2003), Interaction between the Mid-Atlantic Ridge and the Azores hot spot during the last 85 Myr: Emplacement and rifting of the hot spot-derived plateaus, *Geochem. Geophys. Geosyst.*, *4*(10), 8514, doi:10.1029/2003GC000527.

Girod, M., G. Camus, and Y. Vialette (1971), Sur la présence de tholéiites à l'île St Paul (Océan Indien), *Contrib. Mineral. Petrol.*, *33*, 108–117, doi:10.1007/BF00386109.

Graham, D. W., K. T. M. Johnson, L. Douglas-Priebe, and J. E. Lupton (1999), Hotspot-ridge interaction along the Southeast Indian ridge near Amsterdam and St. Paul islands: Helium isotope evidence, *Earth Planet. Sci. Lett.*, *167*(3–4), 297–310, doi:10.1016/S0012-821X(99)00030-8.

Graham, D. W., J. Blichert-Toft, C. J. Russo, K. H. Rubin, and F. Albarède (2006), Cryptic striations in the upper mantle revealed by hafnium isotopes in Southeast Indian Ridge basalts, *Nature*, *440*, 199–202, doi:10.1038/nature04582.

Gunn, B. M., C. E. Abranson, J. Nougier, N. D. Watkins, and A. Hajash (1971), Amsterdam Island, an isolated volcano in the southern Indian Ocean, *Contrib. Mineral. Petrol.*, *32*, 79–92, doi:10.1007/BF00383052.

Gunn, B. M., N. D. Watkins, W. E. Trzcienski Jr., and J. Nougier (1975), The Amsterdam–St. Paul volcanic province and the formation of low Al tholeiitic andesites, *Lithos*, *8*, 137–149, doi:10.1016/0024-4937(75)90021-3.

Hamelin, B., and C. J. Allègre (1985), Large scale regional units in the depleted upper mantle revealed by an isotope study of the Southwest Indian Ridge, *Nature*, *315*, 196–199, doi:10.1038/315196a0.

Hamelin, B., and C. J. Allègre (1986), Pb-Sr-Nd isotopic data of Indian Ocean ridges: New evidence of large scale mapping of mantle heterogeneity, *Earth Planet. Sci. Lett.*, *76*, 288–298, doi:10.1016/0012-821X(86)90080-4.

Hanan, B. B., and D. W. Graham (1996), Lead and helium isotope evidence from oceanic basalts for a common deep source

of mantle plumes, *Science*, *272*, 991–995, doi:10.1126/science.272.5264.991.

Hanan, B. B., J. Blichert-Toft, D. G. Pyle, and D. M. Christie (2004), Contrasting origin of the upper mantle revealed by hafnium and lead isotopes from the Southeast Indian Ridge, *Nature*, *432*, 91–94, doi:10.1038/nature03026.

Hart, S. R. (1984), A large scale isotope anomaly in the Southern Hemisphere mantle, *Nature*, *309*, 753–757, doi:10.1038/309753a0.

Hart, S. R., J.-G. Schilling, and J. L. Powell (1973), Basalts from Iceland and along the Reykjanes Ridge: Sr isotope geochemistry, *Nat. Phys. Sci.*, *246*, 104–107.

Hart, S. R., J. Blusztain, H. J. P. Dick, P. S. Meyer, and K. Muehlenbachs (1999), The fingerprint of seawater circulation in a 500-meter section of ocean crust gabbro, *Geochim. Cosmochim. Acta*, *63*, 4059–4080, doi:10.1016/S0016-7037(99)00309-9.

Hedge, C., N. Watkins, R. Hildreth, and W. Doering (1973), $^{87}Sr/^{86}Sr$ ratios in basalts from islands in the Indian Ocean, *Earth Planet. Sci. Lett.*, *21*, 29–34, doi:10.1016/0012-821X(73)90222-7.

Hemond, C., N. T. Arndt, U. Lichenstein, A. W. Hofmann, N. Oskarsson, and S. Steinthorsson (1993), The heterogeneous Iceland plume: Nd-Sr-O isotopes and trace element constraints, *J. Geophys. Res.*, *98*, 15,833–15,850.

Hofmann, A. W. (2004), Sampling mantle and heterogeneity through oceanic basalts: Isotopes and trace elements, in *Treatise on Geochemistry*, edited by R. W. Carlson, pp. 61–101, Elsevier, New York.

Hofmann, A. W., and K. P. Jochum (1996), Source characteristics derived from very incompatible trace elements in Mauna Loa and Maun Kea basalts. Hawaii Scientific Drilling Project, *J. Geophys. Res.*, *101*, 11,831–11,839, doi:10.1029/95JB03701.

Hofmann, A. W., K. P. Jochum, M. Seufert, and W. M. White (1986), Nb and Pb in oceanic basalts: New constraints on mantle evolution, *Earth Planet. Sci. Lett.*, *79*, 33–45.

Huang, Y.-M., P. Van Calsteren, and C. J. Hawkesworth (1995), The evolution of the lithosphere in southern Africa: A perspective on the basic granulite xenoliths from kimberlites in South Africa, *Geochim. Cosmochim. Acta*, *59*, 4905–4920, doi:10.1016/0016-7037(95)00335-5.

Ingle, S., D. Weis, S. Doucet, and N. Mattielli (2003), Hf isotope constraints on mantle sources and shallow-level contaminants during Kerguelen hot spot activity since ~120Ma, *Geochem. Geophys. Geosyst.*, *4*(8), 1068, doi:10.1029/2002GC000482.

Ito, G., J. Lin, and C. W. Gable (1997), Interaction of mantle plumes and migrating mid-ocean ridges: Implications for the Galápagos plume-ridge system, *J. Geophys. Res.*, *102*, 15,403–15,417, doi:10.1029/97JB01049.

Ito, G., J. Lin, and D. Graham (2003), Observational and theoretical studies of the dynamics of mantle plume-mid-ocean ridge interaction, *Rev. Geophys.*, *41*(4), 1017, doi:10.1029/2002RG000117.

Janin, M. (2010), Le plateau d'Amsterdam–St. Paul: Caractérisation du point chaud éponyme et évolution de son interaction avec la dorsale sud est indienne, PhD dissertation, Univ. of Brest, Brest, France.

Janin, M., X. Hémond, and M. Maia (2010), Amsterdam–St. Paul hotspot history, in *Iceland in the Northern Central Atlantic: Hotspot, Sea Currents and Climatic Change*, pp. 142–143, Cent. Natl. de Rech. Sci., Plouzané, France.

Janin, M., C. Hémond, H. Guillou, M. Maia, K. T. M. Johnson, C. Bollinger, C. Liorzou, and A. Mudhoklar (2011), Hot spot activity and tectonic settings near Amsterdam–St. Paul plateau (Indian Ocean), *J. Geophys. Res.*, *116*, B05206, doi:10.1029/2010JB007800.

Janney, P. E., A. P. LeRoex, and R. W. Carlson (2005), Hafnium isotope and trace element constraints on the nature of mantle heterogeneity beneath the central southwest Indian ridge, *J. Petrol.*, *46*(12), 2427–2464, doi:10.1093/petrology/egi060.

Johnson, K. T. M., D. W. Graham, K. H. Rubin, K. Nicolaysen, D. S. Scheirer, D. W. Forsyth, E. T. Baker, and L. M. Douglas-Priebe (2000), Boomerang Seamount: The active expression of the Amsterdam–St. Paul hotspot, Southeast Indian Ridge, *Earth Planet. Sci. Lett.*, *183*, 245–259, doi:10.1016/S0012-821X(00)00279-X.

Johnson, M. C., and T. Plank (1999), Dehydration and melting experiments constrain in the fate of subducted sediments, *Geochem. Geophys. Geosyst.*, *1*(12), 1007, doi:10.1029/1999GC000014.

Kamenetsky, V. S., R. Maas, M. D. Normal, I. Cartwright, and A. A. Epyve (2001), Remnants of Gondwanan continental lithosphere in oceanic upper mantle: Evidence from the South Atlantic Ridge, *Geology*, *29*, 243–246, doi:10.1130/0091-7613(2001)029<0243:ROGCLI>2.0.CO;2.

Kay, R. W., and S. M. Kay (1993), Delamination and delamination magmatism, *Tectonophysics*, *219*, 177–189, doi:10.1016/0040-1951(93)90295-U.

Kelley, K. A., T. Plak, L. Farr, J. Ludden, and H. Staudigel (2005), Subduction cycling of U, Th and Pb, *Earth Planet. Sci. Lett.*, *234*, 369–383.

Kempton, P. D., J. A. Pearce, T. L. Barry, J. G. Fitton, C. Langmuir, and D. M. Christie (2002), Sr-Nd-Pb-Hf isotopes results from ODP Leg 187: Evidences for mantle dynamics of the Australian-Antarctic Discordance and origin of the Indian MORB source, *Geochem. Geophys. Geosyst.*, *3*(12), 1074, doi:10.1029/2002GC000320.

Langmuir, C. H., R. D. Vocke, and G. N. Hanson (1978), A general mixing equation with applications to Icelandic basalts, *Earth Planet. Sci. Lett.*, *37*, 380–392, doi:10.1016/0012-821X(78)90053-5.

Le Bas, M. J., R. W. Le Maitre, and A. R. Woolley (1992), The construction of the Toral Alkali-Silica chemical classification of volcanic rocks, *Mineral. Petrol.*, *46*(1), 1–22, doi:10.1007/BF01160698.

Leeman, W. P., M. A. Menziès, D. J. Matty, and G. F. Embry (1985), Strontium, neodymium and lead isotopic compositions of deep crustal xenoliths from the Snake River Plain: Evidence for the Archean basement, *Earth Planet. Sci. Lett.*, *75*, 354–368, doi:10.1016/0012-821X(85)90179-7.

LeRoex, A. P., H. J. B. Dick, and R. L. Fischer (1989), Petrology and geochemistry of MORB from 25°E to 46°E along the Southwest Indian Ridge: Evidence for contrasting styles of mantle enrichment, *J. Petrol.*, *30*, 947–986.

Mahoney, J. J., A. P. LeRoex, Z. Peng, R. L. Fisher, and J. H. Natland (1992), Southwestern limits of Indian ocean ridge mantle and origin of low $^{206}Pb/^{204}Pb$ mid-ocean ridge basalt: Isotope systematic of the central southwest Indian ridge (17°–50°), *J. Geophys. Res.*, *97*, 19,771–19,790, doi:10.1029/92JB01424.

Mahoney, J. J., W. M. White, B. G. J. Upton, C. R. Neal, and R. A. Scrutton (1996), Beyond EM-1: Lavas from Afanasy-Nikitin Rise and the Crozet Archipelago, Indian Ocean, *Geology*, *24*, 615–618.

Mahoney, J. J., D. W. Graham, D. M. Christie, K. T. M. Johnson, L. S. Hall, and L. Vonderhaar (2002), Between a hotspot and a cold spot: Isotopic variations along the southeast Indian ridge asthenosphere, 86°E–118°E, *J. Petrol.*, *43*, 1155–1176, doi:10.1093/petrology/43.7.1155.

Maia, M., et al. (2000), The Pacific-Antarctic Ridge-Foundation hotspot interaction: A case study of a ridge approaching a hot spot, *Mar. Geol.*, *167*, 61–84, doi:10.1016/S0025-3227(00)00023-2.

Maia, M., C. Hémond, and P. Gente (2001), Contrasted interactions between plume, upper mantle, and lithosphere: Foundation chain case, *Geochem. Geophys. Geosyst.*, *2*(7), 1028, doi:10.1029/2000GC000117.

Maia, M., et al. (2008), Evolution of the Saint Paul Amsterdam Plateau in the Last 10 m.y., *Eos Trans. AGU*, *89*(53), Fall Meet. Suppl., Abstract T54B-06.

Maia, M., et al. (2011), Building of the Amsterdam–St. Paul plateau: A 10 Myr history of a ridge-hotspot interaction and plume pulses, *J. Geophys. Res.*, *116*, B09104, doi:10.1029/2010JB007768.

Manhes, G., J. F. Minster, and C. Allègre (1978), Comparative U-Th-Pb and Rb-Sr study of the St Severin amphoterite: Consequences for early solar system chronology, *Earth Planet. Sci. Lett.*, *39*, 14–24, doi:10.1016/0012-821X(78)90137-1.

McDonough, W. F., and S. S. Sun (1995), The composition of the Earth, *Chem. Geol.*, *120*, 223–253, doi:10.1016/0009-2541(94)00140-4.

Meyzen, C. M., J. N. Ludden, E. Humler, B. Luais, M. J. Toplis, C. Mével, and M. Storey (2005), New insights into the origin and distribution of the DUPAL isotope anomaly in the Indian mantle from MORB of the Southwest Indian Ridge, *Geochem. Geophys. Geosyst.*, *6*, Q11K11, doi:10.1029/2005GC000979.

Müller, R. D., J.-Y. Royer, and L. A. Lawver (1993), Revised plate motions relative to the hotspots from combined Atlantic and Indian Ocean hotspot tracks, *Geology*, *21*, 275–278.

Nicolaysen, K. P., F. A. Frey, J. J. Mahoney, K. T. M. Johnson, and D. W. Graham (2007), Influence of the Amsterdam/St. Paul hotspot along the Southeast Indian Ridge between 77° and 88°E: Correlations of Sr, Nd, Pb and He isotopic variations with ridge segmentation, *Geochem. Geophys. Geosyst.*, *8*, Q09007, doi:10.1029/2006GC001540.

Patchett, P. J., W. M. White, H. Feldmann, S. Kielinczuk, and A. W. Hofmann (1984), Hafnium/rare earth element fractionation in the sedimentary system and crustal recycling into the Earth's mantle, *Earth Planet. Sci. Lett.*, *69*, 365–378, doi:10.1016/0012-821X(84)90195-X.

Plank, T., and C. H. Langmuir (1998), The chemical composition of subducting sediment and its consequences for the crust and the mantle, *Chem. Geol.*, *145*, 325–394.

Putirka, K. D., M. D. Kuntz, D. M. Unruh, and N. Vaid (2009), Magma evolution and ascent at the craters of the moon and neighboring volcanic fields, southern Idaho., USA: Implications for the evolution of polygenetic and monogenetic volcanic fields?, *J. Petrol.*, *50*, 1639–1665, doi:10.1093/petrology/egp045.

Regelous, M., Y. Niu, W. Abouchami, and P. R. Castillo (2009), Shallow origin for South Atlantic Dupal Anomaly from lower continental crust: Geochemical evidence from the mid-Atlantic ridge at 26°S, *Lithos*, *112*, 57–72, doi:10.1016/j.lithos.2008.10.012.

Reinisch, R. (1909), Gesteine von St. Paul und Neu Amsterdam, in *Deutsch Südpolar-Expedition 1901–1903. Im Auftrage des Reichsamtes Des Innern hrsg. P.I. (Leiter der Expedition): Erich Von Drygalsky. Bd II (Kartographie, Geologie), Heft 5*, pp. 385–398, G. Reimer, Berlin.

Rekhämper, M., and A. W. Hofmann (1997), Recycled ocean crust and sediment in Indian Ocean MORB, *Earth Planet. Sci. Lett.*, *147*, 93–106, doi:10.1016/S0012-821X(97)00009-5.

Ribe, N. M., and W. L. Delattre (1998), The dynamics of plume-ridge interaction—III. The effects of ridge migration, *Geophys. J. Int.*, *133*, 511–518, doi:10.1046/j.1365-246X.1998.00476.x.

Richard, P., N. Shimizu, and C. J. Allegre (1976), $^{143}Nd/^{146}Nd$, a natural tracer: An application to oceanic basalts, *Earth Planet. Sci. Lett.*, *31*(2), 269–278, doi:10.1016/0012-821X(76)90219-3.

Rooney, T. O., B. Hanan, D. W. Graham, T. Furman, J. Blichert-Toft, and J. G. Schilling (2012), Upper mantle pollution during Afar Plume–Continental Rift interaction, *J. Petrol.*, *53*(2), 365–389, doi:10.1093/petrology/egr065.

Royer, J. Y., and R. Schlich (1988), Southeast Indian Ridge between the Rodriguez Triple Junction and the Amsterdam and St. Paul Islands: Detailed kinematics for the past 20 m.y., *J. Geophys. Res.*, *93*(B11), 13,524–13,550, doi:10.1029/JB093iB11p13524.

Rudnick, R. L., and D. M. Fountain (1995), Nature and composition of the continental crust: A lower crustal perspective, *Rev. Geophys.*, *33*, 267–309, doi:10.1029/95RG01302.

Rudnick, R. L., and S. Gao (2003), Composition of the continental crust, in *Treatise in Geochemistry*, vol. 3, *The Crust*, edited by R. L. Rudnick, pp. 1–64, Elsevier, Amsterdam.

Rudnick, R. L., and S. L. Goldstein (1990), The Pb isotopic compositions of lower crustal xenoliths and the evolution of lower crustal crust Pb, *Earth Planet. Sci. Lett.*, *98*, 192–207, doi:10.1016/0012-821X(90)90059-7.

Rudnick, R. L., W. F. McDonough, M. T. McCulloch, and S. R. Taylor (1986), Lower crustal xenoliths from Queensland, Australia: Evidence for deep crustal assimilation and fractionation of continental basalts, *Geochim. Cosmochim. Acta*, *50*, 1099–1115, doi:10.1016/0016-7037(86)90391-1.

Schilling, J.-G. (1991), Fluxes and excess temperatures of mantle plumes inferred from their interaction with migrating mid-ocean ridges, *Nature*, *352*, 397–403, doi:10.1038/352397a0.

Searle, R. C., J. A. Keeton, R. B. Owens, R. S. White, R. Mecklenburgh, B. Parsons, and S. M. Lee (1998), The Reykjanes Ridge: Structure and tectonics of a hot-spot-influenced, slow-spreading ridge, from multibeam bathymetry, gravity and magnetic investigations, *Earth Planet. Sci. Lett.*, *160*, 463–478, doi:10.1016/S0012-821X(98)00104-6.

Sobolev, A. V., A. W. Hofmann, and I. K. Nikogosian (2000), Recycled oceanic crust observed in 'ghost plagioclase' within the source of Mauna Loa lavas, *Nature*, *404*, 986–990, doi:10.1038/35010098.

Stracke, A., M. Bizimis, and V. J. M. Salters (2003), Recycling oceanic crust: Quantitative constraints, *Geochem. Geophys. Geosyst.*, *4*(3), 8003, doi:10.1029/2001GC000223.

Stracke, A., A. W. Hofmann, and S. R. Hart (2005), FOZO, HIMU, and the rest of the mantle zoo, *Geochem. Geophys. Geosyst.*, *6*, Q05007, doi:10.1029/2004GC000824.

Tatsumoto, M. (1978), Isotopic composition of lead in oceanic basalt and its implication to mantle evolution, *Earth Planet. Sci. Lett.*, *38*, 63–87, doi:10.1016/0012-821X(78)90126-7.

Tilton, G. R., and B. Bareiro (1980), Origin of lead in Andean calc-alkaline lavas, southern Peru, *Science*, *210*, 1245–1247, doi:10.1126/science.210.4475.1245.

Turcotte, D. L. (1989), Dynamics of recycling, in *Crust/Mantle Recycling at Convergence Zones*, *NATO ASI Ser., Ser. C*,

vol. 258, edited by S. R. Hart and L. Gülen, pp. 245–257, Kluwer Acad., Dordrecht, Netherlands.

Velain, C. (1878), *Description géologique de la presqu'île d'Aden, de la Réunion, des îles St. Paul et Amsterdam*, 536 pp., Hennuyer, Paris.

Vervoort, J. D., P. J. Patchett, J. J. Blichert-Toft, and F. Albarède (1999), Relationships between Lu-Hf and Sm-Nd isotopic systems in the global sedimentary system, *Earth Planet. Sci. Lett.*, *168*, 79–99, doi:10.1016/S0012-821X(99)00047-3.

von Hochstetter, F. (1866), *Geologische betrachtungen während der reise der Osterreichischen fregatte "Novara" (1857–1859). Um die Erde. 2, Bd*, 58 pp., Gerold, Vienna.

Watkins, N. D., and J. Nougier (1973), Excursions and secular variation of the Bruhnes epoch geomagnetic field in the Indian Ocean region, *J. Geophys. Res.*, *78*, 6060–6068, doi:10.1029/JB078i026p06060.

Watkins, N., B. Gunn, J. Nougier, and A. Baski (1974), Kerguelen: Continental fragment or oceanic island, *Geol. Soc. Am. Bull.*, *85*, 201–212.

Watkins, N. D., I. McDougall, and J. Nougier (1975), Paleomagnetism and potassium-argon age of St. Paul Island, southeastern Indian Ocean: Contrasts in geomagnetic secular variation during the Brunhes Epoch, *Earth Planet. Sci. Lett.*, *24*, 377–384, doi:10.1016/0012-821X(75)90144-2.

Weaver, B. L. (1986), Role of the subducted sediment in the genesis of Ocean island basalts: Geochemical evidence from South Atlantic Ocean islands, *Geology*, *14*, 275–278, doi:10.1130/0091-7613(1986)14<275:ROSSIT>2.0.CO;2.

Weaver, B. L. (1991), Trace element evidence for the origin of oceanic basalts, *Geology*, *19*, 123–126.

White, W. M., and J. Patchett (1984), Hf-Nd-Sr isotopes and incompatible element abundances in island Arcs: Implications for magma origins and crust-mantle evolution, *Earth Planet. Sci. Lett.*, *67*, 167–185, doi:10.1016/0012-821X(84)90112-2.

White, W. M., A. W. Hofmann, and H. Puchelt (1987), Isotope geochemistry of Pacific mid-ocean ridge basalts, *J. Geophys. Res.*, *92*, 4881–4893, doi:10.1029/JB092iB06p04881.

Yang, H. J., F. A. Frey, D. Weis, A. Giret, D. Pyle, and G. Michon (1998), Petrogenesis of the flood basalts forming the northern Kerguelen Archipelago: Implications for the Kerguelen plume, *J. Petrol.*, *39*(4), 711–748, doi:10.1093/petroj/39.4.711.